Major-element composition of sediments in terms of weathering and provenance: Implications for crustal recycling

Alex G. Lipp[1], **Oliver Shorttle**[2,3], **Frank Syvret**[4], **Gareth G. Roberts** [1]

[1]Department of Earth Sciences and Engineering, Imperial College London
[2]Department of Earth Sciences, University of Cambridge
[3]Institute of Astronomy, University of Cambridge
[4]Bullard Laboratories, Department of Earth Sciences, University of Cambridge

Key Points:

- Weathering and provenance dominate fine-grained sedimentary elemental composition
- Protolith composition and weathering intensity are determined from a sediment's composition
- The upper continental crust is recycled into the mantle at a rate of $1.47 \pm 1.00 \times 10^{13}$ kg yr^{-1}.

Corresponding author: Alex Lipp, a.lipp18@imperial.ac.uk

Abstract

The elemental composition of sediments is set by the composition of its protolith and modified by weathering, sorting, and diagenesis. An important problem is deconvolving these myriad contributions to a sediment's composition to arrive at meaningful information about processes that operate on the Earth's surface. We approach this problem by developing a predictive and invertible model of sedimentary major-element composition. We compile a dataset of sedimentary rock, river sediment, soil, and igneous rock compositions. By applying principal component analysis to the log-ratio transformed dataset we observe that most of the compositional variation lies in a 2 dimensional subspace. A composition in this plane can be parameterised by linear vectors of igneous evolution and weathering. We thus define a model for sedimentary composition as a linear combination of these two vectors. A 1:1 correspondence is observed between model predictions and independent data not used in calibrating the model. Deviations from the model can mostly be explained by sodium-calcium exchange. Using this approach we show that the major-element composition of the upper continental crust has been modified by weathering, and we calculate the amount of each element that must be lost to sufficiently modify the crustal composition. By extrapolating modern weathering rates over the age of the crust we conclude that a significant amount of weathering restite has not been incorporated into the upper continental crust. This restite has likely been subducted into the mantle indicating a crust-to-mantle recycling rate of $1.47 \pm 1.00 \times 10^{13}$ kg yr^{-1}.

1 Introduction

The elemental composition of fine grained sediments is principally controlled by the composition of the rocks from which they formed (provenance) and subsequent reactions with fluids, which transform these source rocks into solutes and neoformed minerals in the surface environment (weathering) [*Nesbitt*, 1979; *Nesbitt et al.*, 1980; *Taylor*, 1985; *Nesbitt et al.*, 1996]. Sediment composition is further altered during transport by hydrodynamic sorting [*Cullers et al.*, 1987; *Garzanti et al.*, 2009; *Bouchez et al.*, 2011; *von Eynatten et al.*, 2012, 2016], cation exchange with natural waters [*Sayles and Mangelsdorf*, 1977; *Cerling et al.*, 1989] and during burial by reaction with porewater fluids (diagenesis) [*Nesbitt and Young*, 1989; *Fedo et al.*, 1995]. A challenge of sedimentary geochemistry is to identify the contribution of each of these factors to the formation of any given sediment. Then elemental sedimentary compositions be used to derive useful information about past climates, crustal processes and sedimentary source regions.

Unravelling these factors is made harder by the surprisingly unintuitive nature of compositional data. All compositions are subject to the constraints that all components are strictly positive and must sum to a total 'closure' value (e.g., 100%) [*Pawlowsky-Glahn*, 2015a]. These constraints mean that raw compositional data are not euclidean variables meaning that standard statistical techniques cannot be applied to them. If such techniques are used on raw data the results can be misleading [*Buccianti*, 2013]. *Aitchison* [1986] introduced log-ratio transformations of compositional data which allow standard techniques to be applied. Under a log-ratio transformation some important geological processes that determine compositions can be predicted by simple linear trends. This includes weathering [*von Eynatten et al.*, 2003], sorting [*Bloemsma et al.*, 2012] and igneous differentiation [*Ohta and Arai*, 2007]. Furthermore, *Ohta and Arai* [2007] indicate that the majority of compositional variation in a large dataset of soils can be explained considering only two processes, weathering and igneous differentiation. These findings suggest that despite apparent complexity, sedimentary compositions are predictable and can be described by considering only a relatively small number of processes.

In this study we build on these advances to create a general model for the composition of fine-grained sediments in terms of the composition of the rocks from which they derive, and the weathering processes that modify them. First, we compile a dataset of major-element

compositions from fine-grained sedimentary rocks, river muds, and soils. This dataset is assumed to be a representative population of the range of possible sedimentary compositions. To constrain the compositional trends of weathering and igneous differentiation we gather data from an individual soil profile and an igneous rock suite respectively. Using principal component analysis on the log-ratio transformed sediment compositions we simplify this dataset of seven different major-element oxides down to the compositional vectors that contain significant variance. From this work we derive a 2 dimensional model which explains the majority of the total variability in the dataset of sediment compositions. The fitness of this model is then evaluated by analysing residuals between the theoretical and observed sedimentary compositions. Finally, we demonstrate the utility of our model by analysing the major-element composition of the upper continental crust (UCC) in terms of the processes that have helped form it.

2 Data

All elements in this study are represented as weight percent (wt%) oxides (SiO_2, Al_2O_3, Fe_2O_3, MgO, Na_2O, CaO, K_2O), where Fe_2O_3 represents total iron. Zeros in compositional data prevent the use of log-ratio transformations [*Martín-Fernández et al.*, 2003]. To overcome this problem we exclude samples where a zero is present (e.g., below detection limit, or not analysed) in any oxide. Given that zero values are rare for major-elements, this exclusion is unlikely to bias our results. We also exclude incomplete compositions.

The composition of upper continental crust (UCC) is a useful reference point to compare to other compositions (e.g. weathering products, igneous protoliths) and calculated compositional vectors (e.g. weathering and protolith trends). Moreover, determining where the composition of UCC sits within the range of compositions observed is a useful guide to the processes that have generated and modified UCC. We take the composition of UCC defined by *Rudnick and Gao* [2003].

2.1 Sedimentary Rocks

We compiled 2822 major-element compositions of fine-grained sedimentary rocks. To minimise the effect of grain-size we include only fine-grained sediments. We note that in most cases grain-size, if noted at all, is given qualitatively in the original source (e.g.,"fine-grained", "mudrock" etc.) and that quantitative grain-size data is rarely available. To minimise the effect of carbonate contamination we exclude samples that are reported to contain carbonate. However, because it is not always possible to detect carbonate without a mineralogical analysis we also exclude samples with a CaO of > 10wt%.

2.2 River Sediments

Pre-existing river sediment compilations [*Martin and Meybeck*, 1979; *Gaillardet et al.*, 1999; *Viers et al.*, 2009] and additional literature data are compiled to produce a dataset of 261 samples. As a qualitative control for grain-size we only include suspended sediment compositions and deposited sediments described as fine-grained (e.g.,"bank muds") or those that were filtered to exclude the coarse fraction (e.g., > 150 μm). Data collected from river depth-profiles are used to explore the compositional effect of grain-size [*Bouchez et al.*, 2011, 2012; *Lupker et al.*, 2012]. These depth profiles sample river sediment at different heights in the water column where sediment grain-size varies systematically.

2.3 Soils

A geochemical dataset of soil compositions was compiled from sources listed in *Ohta and Arai* [2007] who recorded soil data from a range of different climatic zones and a diverse suite of igneous rock protoliths. To define a compositional trend for weathering it is neces-

sary to isolate this process from other factors which modify sediment composition. Samples taken from different depths of a single soil profile affected only by differing amounts of weathering can be used to constrain the weathering trend. One such example is the Toorongo Granodiorite weathering profile in Southern Australia. Using data from *Nesbitt and Markovics* [1997], *von Eynatten et al.* [2003] found that the compositional trend defined by samples from this profile is able to reproduce the compositional variability of river sediments from across the globe. This result suggests that this trend might be a globally applicable weathering signal. Consequently, we use this same dataset to define the compositional trend of weathering. It contains 15 samples collected at different locations in the Toorongo weathering profile. The samples range from pristine granodiorite at the centre of a corestone to progressively more altered samples and highly altered material infilling joints.

2.4 Igneous Rocks

We also want to isolate the compositional trend defined by evolution from a mafic primary melt to an evolved felsic melt. To do this we compile igneous rock compositions from Crater Lake (Mount Mazama) in Oregon. Crater Lake is a volcanic cluster with well studied igneous petrology, and showing a wide range of igneous rocks. Making the assumption that all the igneous rocks from Crater Lake are derived from an identical primary melt which has not varied in time, the only process differentiating the compositions is igneous evolution. The compositional trend then will represent igneous evolution. Data were obtained from the GEOROC (http://georoc.mpch-mainz.gwdg.de/georoc/)) database, which was queried with the location names "MOUNT MAZAMA(CRATER LAKE), OREGON" or "MOUNT MAZAMA, OREGON" for whole rock analyses of major-elements. Samples with incomplete compositions were removed to yield 135 samples of major-element compositions ranging from basalt to rhyolite.

3 Statistical methods

3.1 Centred Log-Ratio Transformation

Formally we define a composition $\mathbf{x}$ as $[x_1, x_2, ..., x_D]$ where

$$x_i > 0\,, \quad i = 1\,, 2\,, \ldots\,, D\,; \quad \sum_{i=1}^{D} x_i = \kappa$$

and κ indicates the closure value to which compositions are normalised for inter-sample comparison. In this study we use $\kappa = 100$ because we present compositions in terms of percentages. We utilise the centred log-ratio (clr) transformation defined by *Aitchison* [1986]. The clr transformation transforms a D-part compositional vector into a vector of D dimensions in a real space. Each initial component of a composition (e.g., CaO) corresponds to a clr coefficient, indicated by the notation c(x_i), e.g., c(CaO). The transformation is described by the following expression

$$\mathbf{x}' = clr(\mathbf{x})$$
$$x_i' = \ln\left(\frac{x_i}{g(\mathbf{x})}\right)$$

with $g(\mathbf{x})$ representing the geometric, in contrast to the arithmetic, mean of $\mathbf{x}$ given by

$$g(\mathbf{x}) = \left(\prod_{i=1}^{D} x_i\right)^{1/D}\,.$$

The inverse operation to recover the initial composition $\mathbf{x}$ from the clr coefficients $\mathbf{x}'$ is simply

$$\mathbf{x} = clr^{-1}(\mathbf{x}') = C(\exp\left(clr(\mathbf{x})\right))$$

where C is the closure operation, indicating normalisation to the closure value κ.

Table 1. An example of the centred log-ratio transformation using the composition of UCC [*Rudnick and Gao*, 2003]. The first row contains the wt% oxide components, normalised to 100 %. The second row are the clr coordinates of this composition.

	SiO_2	Al_2O_3	Fe_2O_3	MgO	Na_2O	CaO	K_2O
UCC	66.8	15.4	5.61	2.49	3.28	3.60	2.81
c(UCC)	2.33	0.869	−0.142	−0.957	−0.681	−0.587	−0.836

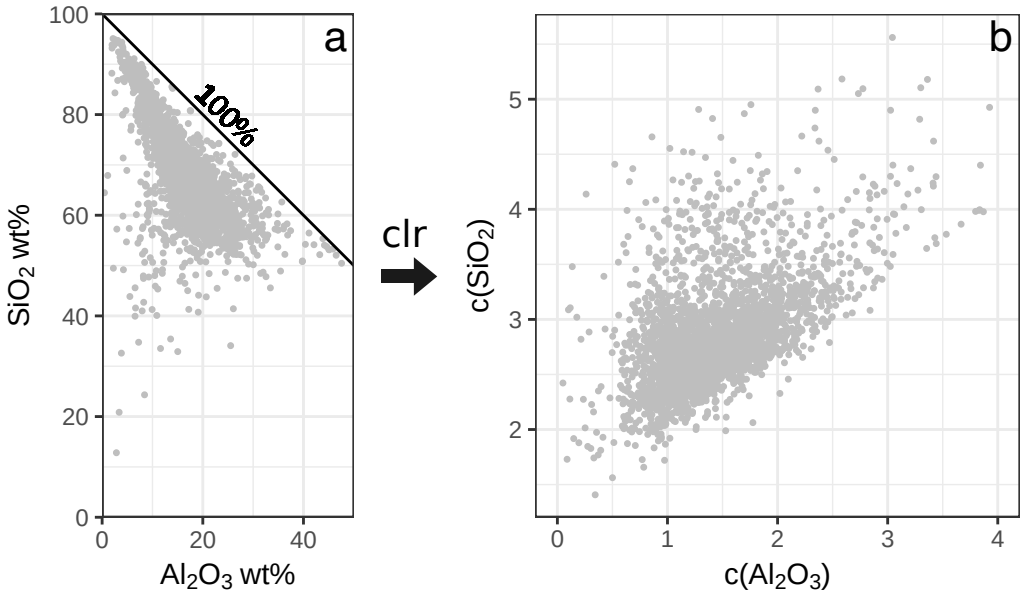

Figure 1. (a) Crossplot of wt% SiO_2 and Al_2O_3 for the compiled sedimentary rock compositions, normalised to 100%. The constant sum constraint means SiO_2 and Al_2O_3 can never sum to more than 100%, indicated by the black line. This constraint prevents application of standard statistical techniques. (b) Cross plot of centred log-ratio, clr, SiO_2 and Al_2O_3 coordinates from the same dataset as Figure 1a. Unlike the raw wt% data, the clr coordinates can occupy the entire sample space without restrictions, in this case highlighting the correlation between Si and Al, as opposed to the apparent negaive correlation in the raw data.

As an example, Table 1 shows the raw composition (in wt%) and also the clr coordinates for the composition of UCC. The coordinates represent the relative, not absolute, variation of each component with respect to the geometric mean of the composition, which in this instance is 6.47 wt%. Components with values greater than the geometric mean have positive coordinates (e.g., SiO_2). Components with values less than the geometric mean have negative coordinates (e.g., MgO). The value of the clr coordinates is independent of the closure value chosen.

The clr transformation has two particularly important characteristics. Firstly, it removes the effect of the closure constraint which precludes the application of statistical procedures designed for euclidean variables. For example, Figure 1a shows the raw SiO_2 and Al_2O_3 wt% of the compiled sedimentary rock composition dataset plotted against each other. Because of the closure constraint SiO_2 and Al_2O_3 can never sum to more than 100 %, meaning the points in Figure 1a can never lie above the line labelled 100 %. In contrast, the clr coordinates can take any value and can occupy the entire space shown in Figure 1b. Secondly, clr coordinates are sensitive to relative not absolute variation. To demonstrate the importance of relative variation consider the following example: SiO_2 in a suite of samples varies from 60 to 65 wt% and CaO varies from 1 to 6 wt%. Both SiO_2 and CaO have an absolute variance of 5 wt%, but SiO_2 has a relative variance of 1.08, in contrast to 5 for CaO. In this instance the relative variance is important, and this is captured in the clr coordinates.

We use the clr transformation and inverse as implemented in R by the package compositions [*van den Boogaart et al.*, 2015; *R Core Team*, 2018].

3.2 Principal Component Analysis

In many datasets variables often covary in response to some underlying process. Because of these correlations it is frequently possible to simplify datasets in terms of fewer variables than the initial dataset. Principal Component Analysis (PCA) does this by rotating the dataset onto a series of orthogonal vectors along which the variance is maximised. These are known as principal components. By analysing the components which contain the most variance we simplify the dataset to contain only the most important variations. If PCA is successful in reducing the dimensionality of a dataset, a large amount of variance will be contained on a small number of principal components. Dimension reducing techniques such as PCA are useful ways to visualise compositional datasets of many parts and are increasingly used in the geosciences, for example in sedimentary provenance analysis [*Aitchison*, 1983; *Aitchison and J. Egozcue*, 2005; *Vermeesch and Garzanti*, 2015]. We apply PCA to the clr transformed dataset via eigenvalue decomposition using the princomp function in R [*R Core Team*, 2018].

4 Results

After applying PCA to the clr transformed sedimentary rock compositions we find that 84% of the total variation is contained within the first three principal components (Figure 2a). This means the dataset can be visualised in 3 dimensions with minimal (16%) loss of information (Figure 2b). An interactive 3D version of these figures (Figure 2b, Figure 3) which are easier to interpret than the 2D projections shown here, can be found in the Supporting Information.

From this visualisation we draw the following key observations:

- The compositional trend of igneous evolution, as defined by the Crater Lake suite, is approximately linear in clr space (green circles in Figure 2b).
- The compositional trend of weathering defined by the Toorongo soil profile is also approximately linear in clr space (pink circles in Figure 2b).

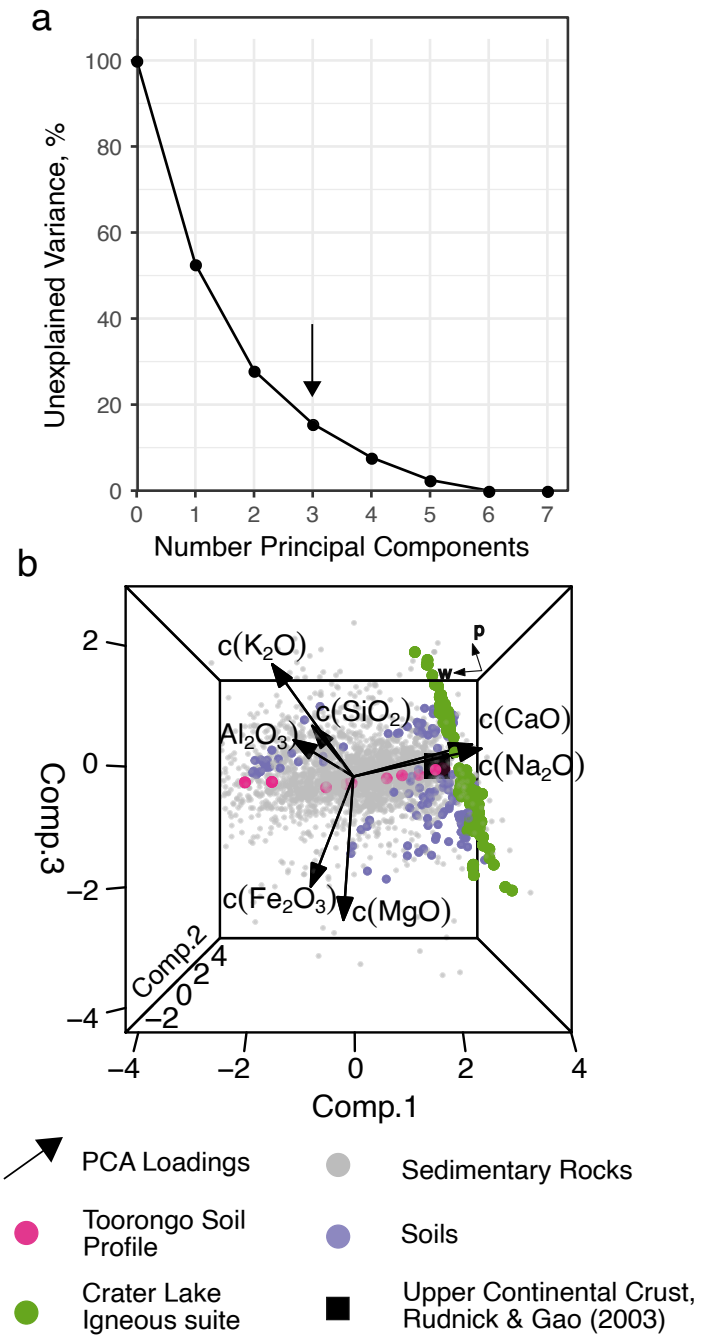

Figure 2. (a) "Scree plot" which displays the amount of variance contained on principal components of sedimentary rock compositional database. Arrow indicates the first three components (displayed in Figure 2b and Figure 3b-e) which contain 84% of the total variance. (b) One view of the first three principal components of sedimentary rock dataset. Note the linearity of the Crater Lake Igneous suite and the Toorongo Soil profile, this panel is also shown in Figure 3c.

- Soils (blue circles), sedimentary rocks (grey circles), and river sediments (pink circles) are translated parallel to the Toorongo soil profile trend from a point of origin along the Crater Lake igneous rock trend (Figure 3b,c). This offset corresponds to decreasing c(Na_2O) and c(CaO).
- The sediments are also distributed parallel to the igneous evolution trend corresponding to increasing c(K_2O), c(SiO_2), c(Al_2O_3) and c(Na_2O) relative to other components (Figure 3a,c).
- If a plane is fit through the point defined by UCC (black square) that is parallel to the igneous and weathering trends (e.g., the blue plane in Figure 3) modern day soils lie close to this plane, but sedimentary rocks deviate from it (Figure 3a,b). This deviation involves an increase in c(Na_2O) and a decrease in c(CaO).
- River sediments occupy a similar space to sedimentary rocks but are only present on the side of the fitted plane higher in c(CaO) (Figure 3d).
- Present day UCC lies close to the igneous trend, but translated a small amount along the weathering trend (Figure 3c).

5 A model for sediment composition

Based on the observations presented in the previous section we derive a predictive model for the composition of a sediment. The structure of the data shown in Figure 3 indicates that sedimentary composition is strongly controlled by the composition of its protolith and alteration during chemical weathering. At this stage we proceed assuming that these are the two most important processes that control sedimentary composition. The validity of this assumption will be subsequently tested by its ability to recover structure from the data.

We define the following equation for a clr transformed sediment composition, $\mathbf{x}'$, in terms of linear unit-length weathering, $\hat{\mathbf{w}}$, and protolith vectors ,$\hat{\mathbf{p}}$, and an orthogonal misfit term, $\mathbf{E}$. Note that the vectors $\hat{\mathbf{w}}$ and $\hat{\mathbf{p}}$ are not required to be orthogonal to each other.

$$\mathbf{x}' = \mathbf{UCC} + \omega\hat{\mathbf{w}} + \psi\hat{\mathbf{p}} + \mathbf{E} \tag{1}$$

This model is visualised in Figure 3a.

	c(SiO_2)	c(Al_2O_3)	c(Fe_2O_3)	c(MgO)	c(Na_2O)	c(CaO)	c(K_2O)
$\hat{\mathbf{w}}$	0.262	0.426	0.160	0.108	−0.522	−0.632	0.200
$\hat{\mathbf{p}}$	0.234	0.098	−0.232	−0.601	0.248	−0.336	0.589
UCC	2.33	0.869	−0.142	−0.957	−0.681	−0.587	−0.836

Table 2. Values of clr vectors used in Equations 1

The vectors $\hat{\mathbf{w}}$ and $\hat{\mathbf{p}}$ must be independently calibrated to the processes they represent, i.e., weathering and provenance respectively. This is done by applying PCA to the Toorongo dataset, for weathering, and Crater Lake dataset, for provenance, and extracting the loadings for the first principal components. These components contain 98 % and 95 % of the total dataset variation, respectively (Table 2).

In Equation 1, ω represents the intensity of weathering experienced by a sediment, and ψ corresponds to the composition of the igneous protolith. The model detailed in Equation 1 allows us to characterise any sediment composition simply in terms of the coefficients ω and ψ. We choose UCC as an origin (i.e., (ψ, ω) co-ordinates of $(0, 0)$) which means that primary igneous rocks have ω less than 0 (i.e., less weathered than UCC), the implications of which are discussed further below. The misfit term $\mathbf{E}$ is the perpendicular distance between $\mathbf{x}'$ and

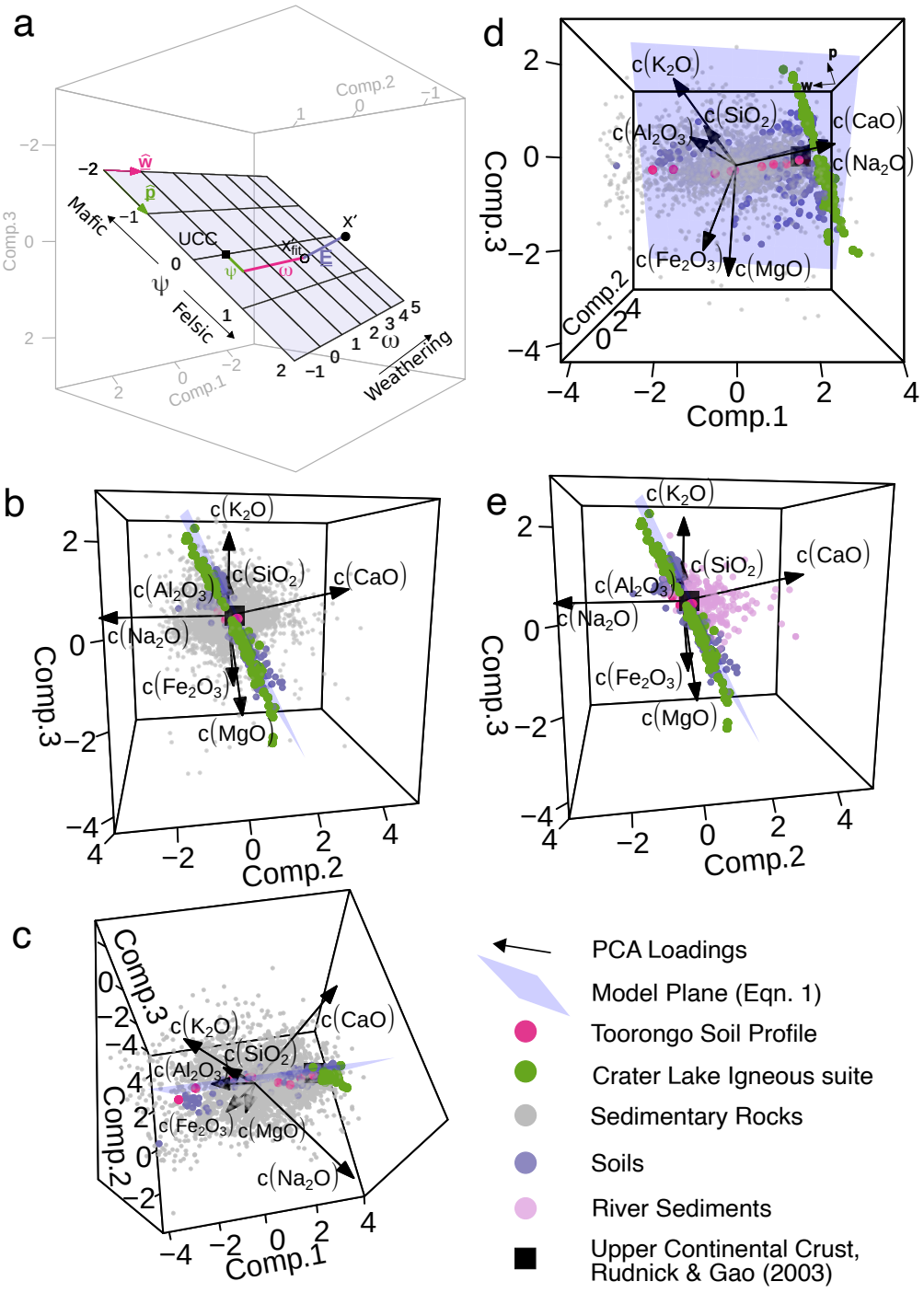
a
Comp.2
Comp.3
Comp.1
Mafic
Felsic
Weathering
UCC
X'
d
Comp.3
Comp.2
Comp.1
c(K2O)
c(SiO2)
c(CaO)
c(Al2O3)
c(Na2O)
c(Fe2O3)
c(MgO)
b
Comp.3
Comp.2
e
Comp.3
Comp.2
c
Comp.3
Comp.2
Comp.1
PCA Loadings
Model Plane (Eqn. 1)
Toorongo Soil Profile
Crater Lake Igneous suite
Sedimentary Rocks
Soils
River Sediments
Upper Continental Crust, Rudnick & Gao (2003)

Figure 3. (a) Visualisation of the model (blue plane) described in Equation 1 in the space defined by the first three principal components of the sedimentary rock database (Figure 3). $\hat{\mathbf{w}}$, and $\hat{\mathbf{p}}$ are unit vectors for weathering and provenance respectively (pink and green arrows). ω and ψ are the coefficients of these vectors which define the position of points on the model plane (shown for $\mathbf{x}'$ with pink and green lines). The origin (ω=0, ψ=0) is defined as the composition of the upper continental crust, UCC (black square). $\mathbf{x}'$ represents a clr transformed composition (filled black circle) and $\mathbf{x}'_{fit}$ the perpendicular projection of this onto the model plane (open circle). $\mathbf{E}$ is the perpendicular distance between $\mathbf{x}'$ and $\mathbf{x}'_{fit}$ (blue line). Highly weathered sediments plot with high ω values. Mafic samples have negative ψ and felsic samples positive ψ, relative to UCC. (b-e) Projection of the different datasets onto the first three principal components of the sedimentary rock dataset. Panels are different perspectives of same projection. For clarity river sediments are excluded from Figure 3a-c but shown in Figure 3d with the same perspective as Figure 3a. Points are compositions and the arrows are the original variable axes with length proportional to variance. The blue plane is the model described in Equation 1 and relates sediment composition to weathering and provenance. Composition of upper continental crust, UCC, taken from *Rudnick and Gao* [2003]. An interactive 3D version of this figure, which is easier to interpret than the 2D projections shown here, can be found in the Supporting Information.

the model plane, (i.e., $\mathbf{E} \cdot \hat{\mathbf{w}} = \mathbf{E} \cdot \hat{\mathbf{p}} = 0$). Factors other than protolith composition and weathering which affect composition will cause the misfit to rise.

5.1 Calculating ω and ψ

We can quantitatively determine the different contributions of weathering and provenance to a sediment's composition by calculating ω and ψ. For a given major-element composition ω and ψ can be determined analytically, as demonstrated below. This solution which calculates the coefficients for any major-element composition has been implemented in R and is freely available (see Acknowledgements for details).

We consider a measured major-element sediment composition $\mathbf{x}$ and the corresponding clr-transformed coordinates $\mathbf{x}'$. We want to find the values of ω and ψ such that:

$$\mathbf{x}' = \omega\hat{\mathbf{w}} + \psi\hat{\mathbf{p}} + \mathbf{E}. \tag{2}$$

The optimal solution to this equation is one where ω and ψ minimise the misfit, $\mathbf{E}$. This minimisation occurs when $\mathbf{E}$ is perpendicular to the plane defined by $\hat{\mathbf{w}}$ and $\hat{\mathbf{p}}$. Thus we have:

$$\hat{\mathbf{w}} \cdot \mathbf{E} = \hat{\mathbf{p}} \cdot \mathbf{E} = 0.$$

$\hat{\mathbf{w}}$ and $\hat{\mathbf{p}}$ are of unit length and not perpendicular to each other, therefore:

$$|\hat{\mathbf{w}}| = |\hat{\mathbf{p}}| = 1; \hat{\mathbf{w}} \cdot \hat{\mathbf{p}} \neq 0.$$

We now define a pair of orthonormal vectors, $\hat{\mathbf{a}}$ and $\hat{\mathbf{b}}$, which lie in the $\hat{\mathbf{p}}$, $\hat{\mathbf{w}}$ plane.

$$\mathbf{a} = \hat{\mathbf{w}} \tag{3}$$

$$\hat{\mathbf{a}} = \frac{\mathbf{a}}{|\mathbf{a}|} \tag{4}$$

$$\mathbf{b} = \hat{\mathbf{p}} - (\hat{\mathbf{a}} \cdot \hat{\mathbf{p}})\hat{\mathbf{a}} \tag{5}$$

$$\hat{\mathbf{b}} = \frac{\mathbf{b}}{|\mathbf{b}|} \tag{6}$$

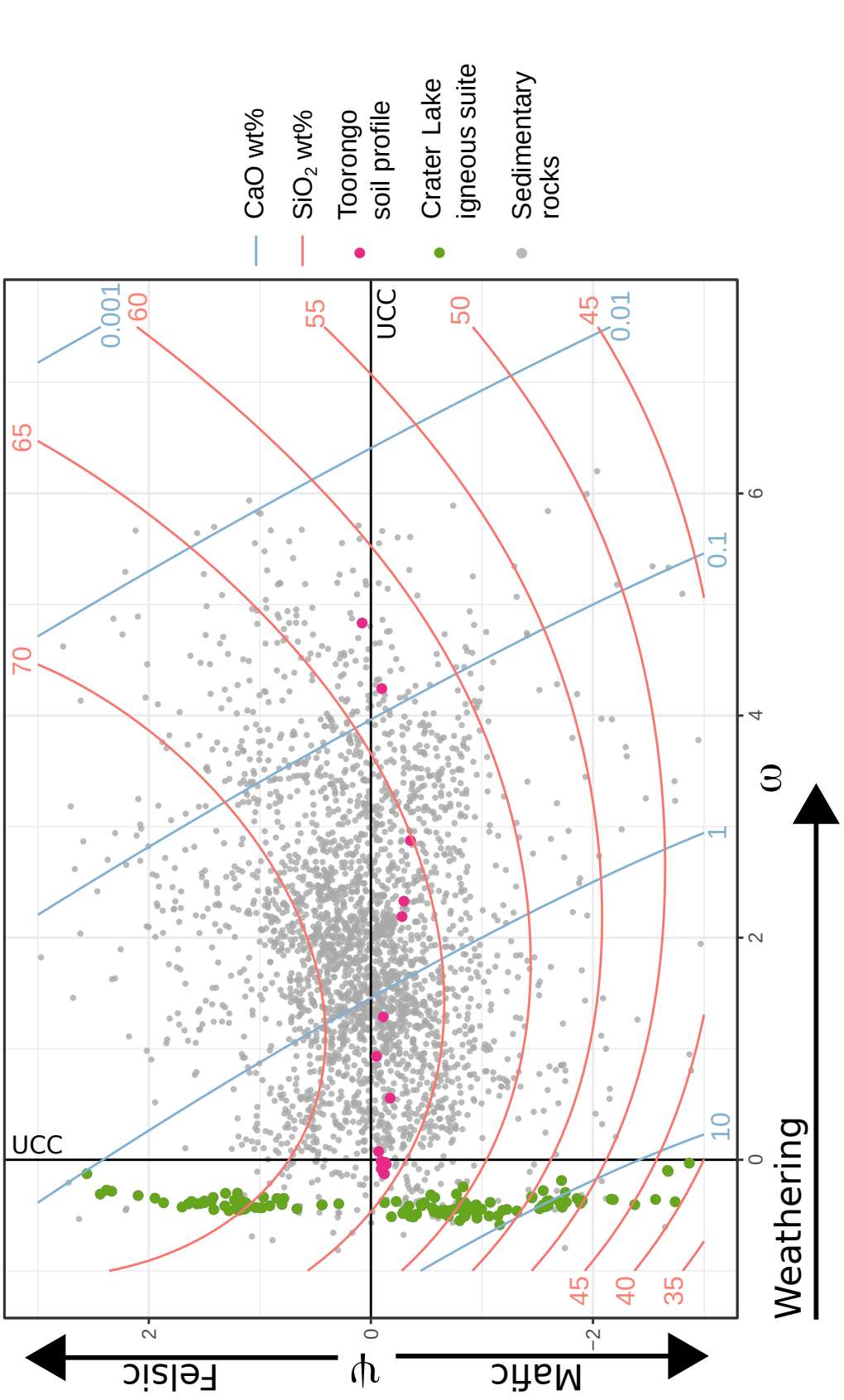

Figure 4. Figure showing the ω and ψ values calculated for the sedimentary rock database by solving Equation 1. Changing the composition of the sediment's protolith acts to move a composition up (more felsic) and down (more mafic). Weathering a sediment causes a composition to move to the right. Green circles are compositions from Crater Lake suite of igneous rocks. Pink circles are compositions from the Toorongo soil profile. Compositional contours are calculated for the model plane (visualised in Figure 3). The origin corresponds to the composition of the upper continental crust, UCC.

We can re-write Equation 2 in terms of these orthonormal vectors as:

$$\mathbf{x}' = \alpha\hat{\mathbf{a}} + \beta\hat{\mathbf{b}} + \mathbf{E} \tag{7}$$

Given that $\hat{\mathbf{a}} \cdot \hat{\mathbf{b}} = \hat{\mathbf{b}} \cdot \mathbf{E} = \hat{\mathbf{a}} \cdot \mathbf{E} = 0$, α and β can be found with:

$$\alpha = \mathbf{x}' \cdot \hat{\mathbf{a}}$$
$$\beta = \mathbf{x}' \cdot \hat{\mathbf{b}}$$

However, the goal is to find ω and ψ. Substituting Equations 3 - 6 into Equation 7 gives:

$$\begin{aligned}\mathbf{x}' &= \alpha\hat{\mathbf{w}} + \frac{\beta}{|\mathbf{b}|}[\hat{\mathbf{p}} - (\hat{\mathbf{w}} \cdot \hat{\mathbf{p}})\hat{\mathbf{w}}] + \mathbf{E} \\ &= [\alpha - \frac{\beta}{|\mathbf{b}|}(\hat{\mathbf{w}} \cdot \hat{\mathbf{p}})]\hat{\mathbf{w}} + \frac{\beta}{|\mathbf{b}|}\hat{\mathbf{p}} + \mathbf{E}\end{aligned} \tag{8}$$

Comparing Equation 8 to Equation 2 we can find ω and ψ by:

$$\omega = \alpha - \frac{\beta}{|\mathbf{b}|}(\hat{\mathbf{w}} \cdot \hat{\mathbf{p}})$$
$$\psi = \frac{\beta}{|\mathbf{b}|}$$

Using the above analytical solution we can calculate the ω and ψ for any major-element composition. The calculated values of ω and ψ for sedimentary rocks are shown in Figure 4. Each point in this $\omega - \psi$ space corresponds uniquely to a composition as indicated by the contours. Projection of samples onto this space allows compositions to be related to weathering intensity and provenance, relative to the reference point of UCC.

6 Evaluation of model

From Equation 1, the modelled clr-vector is simply

$$\mathbf{x}'_{fit} = \mathbf{UCC} + \omega\hat{\mathbf{w}} + \psi\hat{\mathbf{p}}$$

and thus the modelled composition $\mathbf{x}_{fit}$ is simply $clr^{-1}(\mathbf{x}'_{fit})$. Modelled compositions are compared against observed compositions for sedimentary rocks in Figure 5. These compositions lie close to the 1:1 trend, indicating a good fit. Oxides which appear to be poorly fit by the model in this representation (e.g., SiO_2) often have low total variance. In other-words, the variation is poorly explained because there is little variance to explain.

Another way to evaluate the success of the model is shown in Figure 6 for soil samples. This figure demonstrates the effect that changing ω and ψ has in terms of the raw compositional components. The observed and modelled soil values are shown to be well-fitted.

6.1 Coefficients of determination

A useful way to quantify effectiveness of a model is the coefficient of determination, R^2. For a given dataset, the R^2 is the proportion of variance explained by the model relative to the total observed variance of a dataset. It is calculated to be the ratio of the total sum of the squares of modelled variation over the total sum of the squares of observed variance, both relative to the dataset mean.

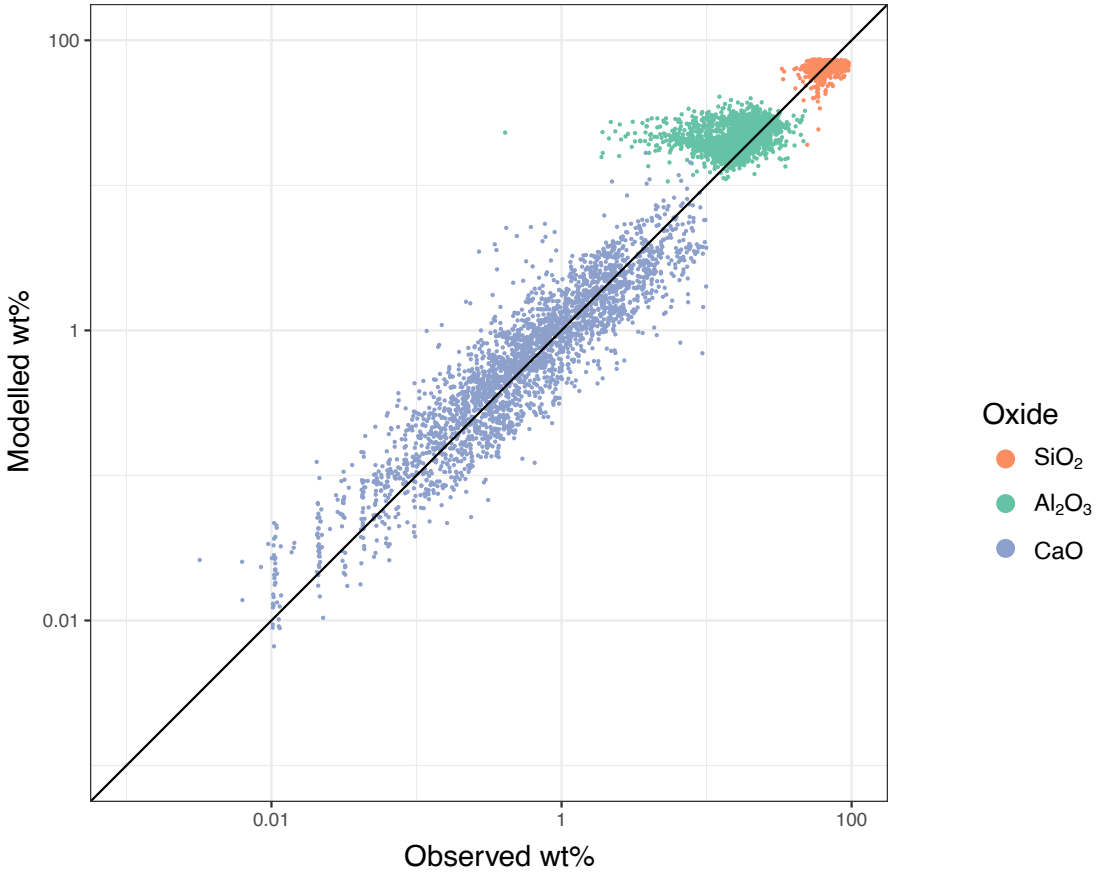

Figure 5. Cross plot of modelled and observed wt% for sedimentary rock compostions. For clarity, only CaO, SiO_2 and Al_2O_3 are shown. Most points lie close to 1:1 line (black line) indicating a good fit. This also indicates the different scales of variance for different elements. CaO varies over 3 orders of magnitude in contrast to SiO_2 and Al_2O_3 which shows minimal variance.

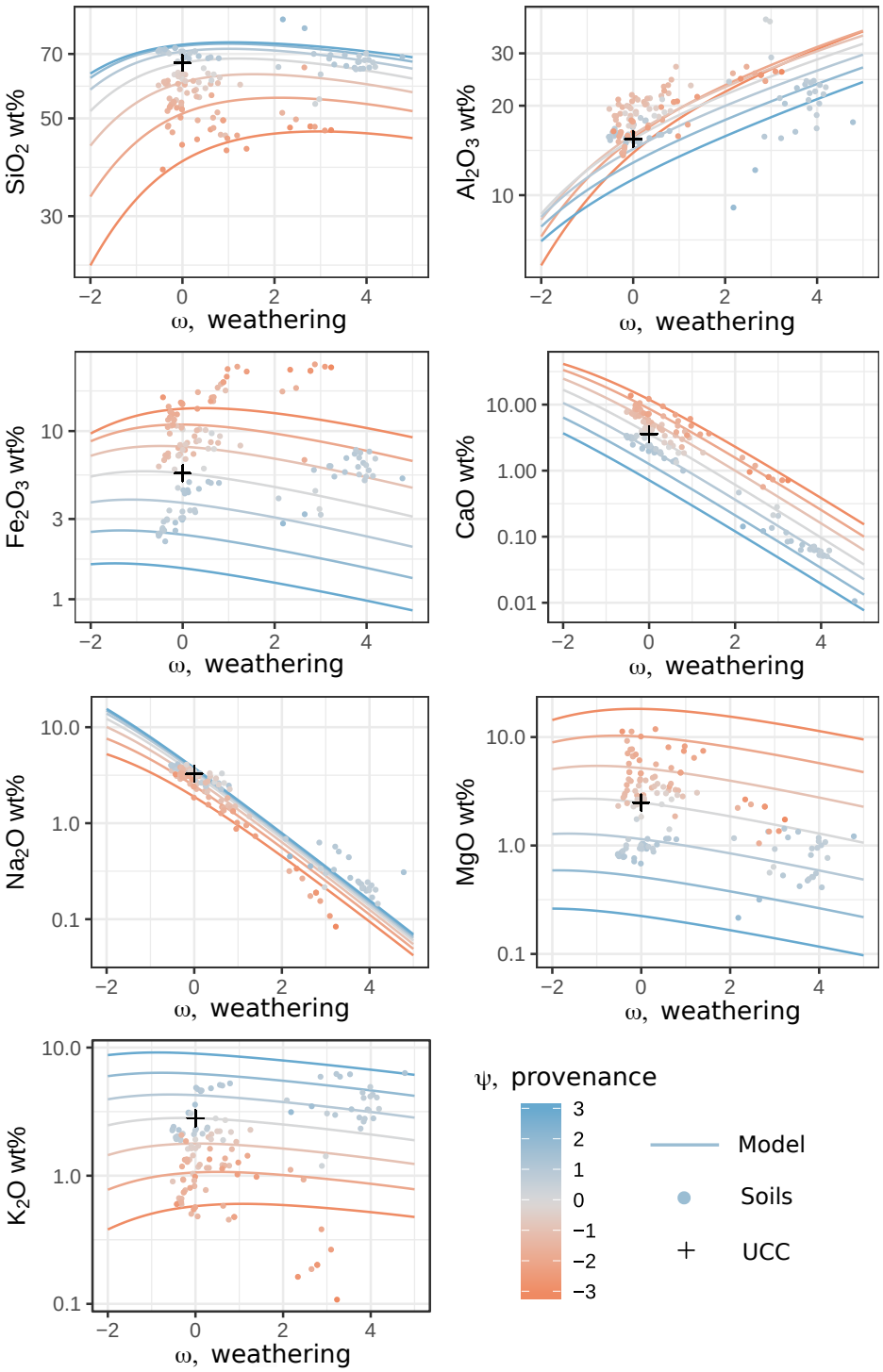

Figure 6. Comparison of modelled vs. observed compositions for soils. Lines indicate contours of ψ for the model plane. Points are observed soil compositions. Colour of point corresponds to the calculated ψ value. If the model accurately predicts the sediment composition the points will lie close to a line of the same colour. This figure demonstrates the effect of varing ψ, provenance, and ω, weathering, on the wt% oxide.

Table 3. Table displaying the calculated R^2 values for the different datasets. The R^2 value is the proportion of the total observed variance that is explained by the model, ranging between 0 and 1.

Dataset	R^2
Soils	0.88
River Sediments	0.67
Sedimentary Rocks	0.59

The R^2 values for different datasets are shown below in Table 3. In all instances the model captures the majority of observed variation. The soil dataset has the highest R^2 value, indicating that our model captures 0.88 of the total variation in soils. River sediments and sedimentary rocks have lower R^2 values consistent with observations of the distribution of the different datasets relative to the model plane in Figure 3. Soils lie close to the plane but the river sediments and the sedimentary rocks both show significant out of plane variation. Of river sediments and sedimentary rocks, the latter shows more out of plane variation consistent with a lower R^2. That these datasets have different coefficients of determination might indicate that some other geological processes are acting on sedimentary compositions. To further investigate this possibility we analyse the misfit between the modelled and observed values, the residuals, for the different datasets.

6.2 Residual Analysis

Analysis of the model residuals indicates the nature of the variation that is not being captured by the model, and may indicate what processes cause the different datasets to have different R^2. For a given $\mathbf{x}'$, the residuals are given by

$$\mathbf{E} = \mathbf{x}' - \mathbf{x}'_{\mathbf{fit}}.$$

Figure 7 indicates that there is a systematic variation of the error magnitude with ω. This variation indicates that the value of $\hat{\mathbf{w}}$ as derived from the Toorongo profile is not perfectly calibrated for representing average weathering. For highly weathered samples the reliability of the calculated value of ψ is less, and may be biased.

This miscalibration is likely due to the fact that it is calibrated at one site. To extract a weathering vector using PCA requires more samples than variables (in this case 7), and we found few profiles where this is the case. In future, it may be possible to derive a consensus value for $\hat{\mathbf{w}}$ from multiple different weathering sites. The value used in this study, however, probably captures most of the important variability. There is no observed systematic variability with changing ψ, indicating that the provenance vector, $\hat{\mathbf{p}}$, is well calibrated.

Kernel Density Estimates of residuals for each element calculated from the sedimentary rocks are shown in Figure 8. For $c(Al_2O_3)$, $c(SiO_2)$ and $c(K_2O)$ the residuals are approximately normally distributed around 0, but this is not the case for the other elements.

Plotting the oxide residuals against each other indicates a series of systematic relationships between the residuals of c(CaO), $c(Na_2O)$, c(MgO) and $c(K_2O)$ (Figure 9). These observations suggest that there is a process that systematically affects the composition of sediments but which is not explicitly accounted for in the model described in Equation 1. We consider two possible processes that might create these trends: calcite addition, and cation exchange.

Equation 1 only considers the siliciclastic portion of a sediment, however detrital and authigenic carbonate minerals, in particular calcite ($CaCO_3$), are important constituents of many sediments. Although addition of calcite adds only calcium to the major elements of a sediment, through the closure constraint this process also affects the observed value of the

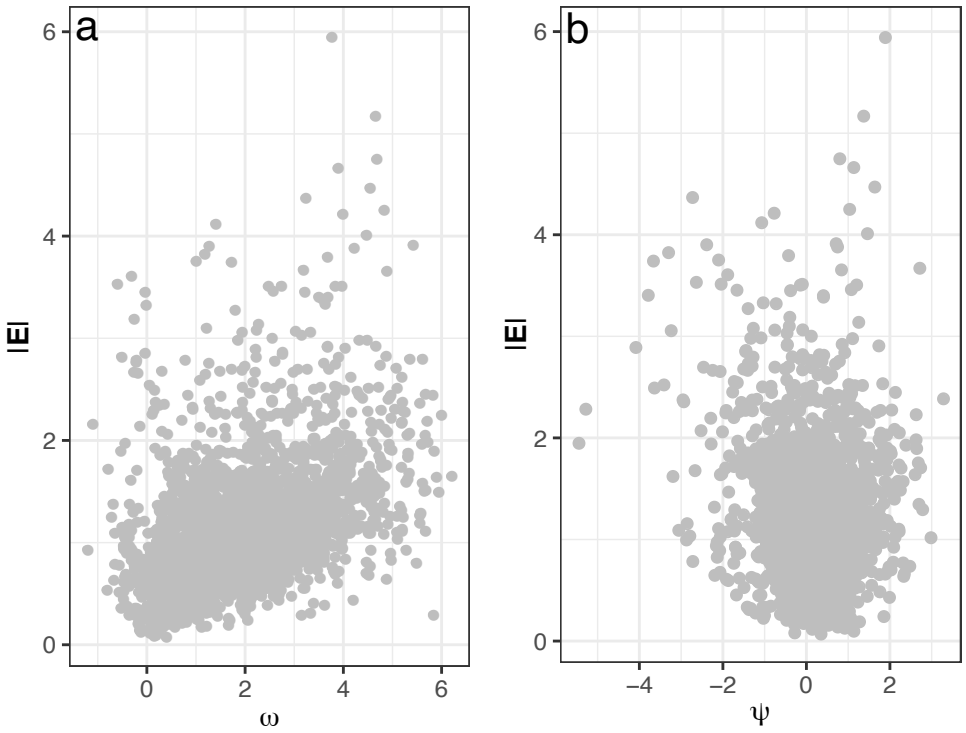

Figure 7. Magnitude of residuals plotted against model coefficients from Equation 1. (a) ω shows weak positive correlation with residual magnitude indicating minor miscalibration of $\hat{\mathbf{w}}$. (b) No relationship observed between ψ and residual magnitude, which indicates well calibrated $\hat{\mathbf{p}}$.

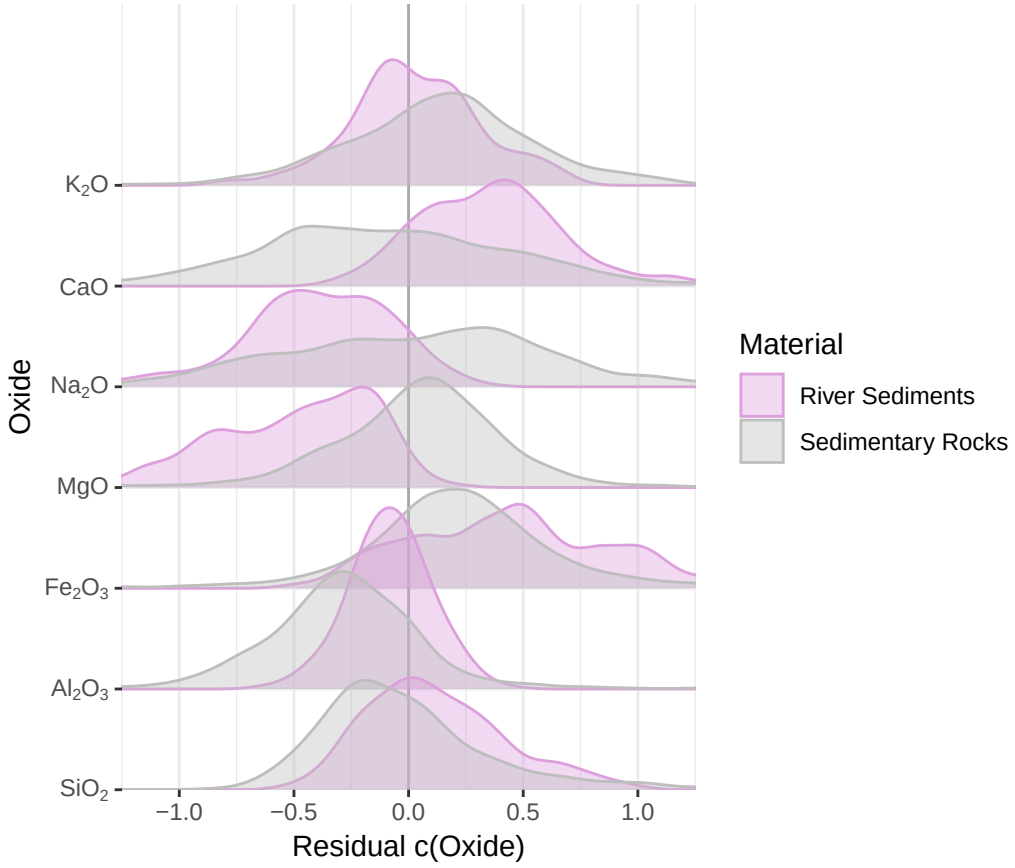

Figure 8. Kernel Density Estimates of residuals, **E**, for each oxide for sedimentary rocks (grey) and river sediments (pink). Vertical grey line emphasises residuals of 0, corresponding to the model plane fitted through UCC. Positive residual indicates greater c(Oxide) than model prediction, and negative residual indicates a lower c(Oxide) than predicted

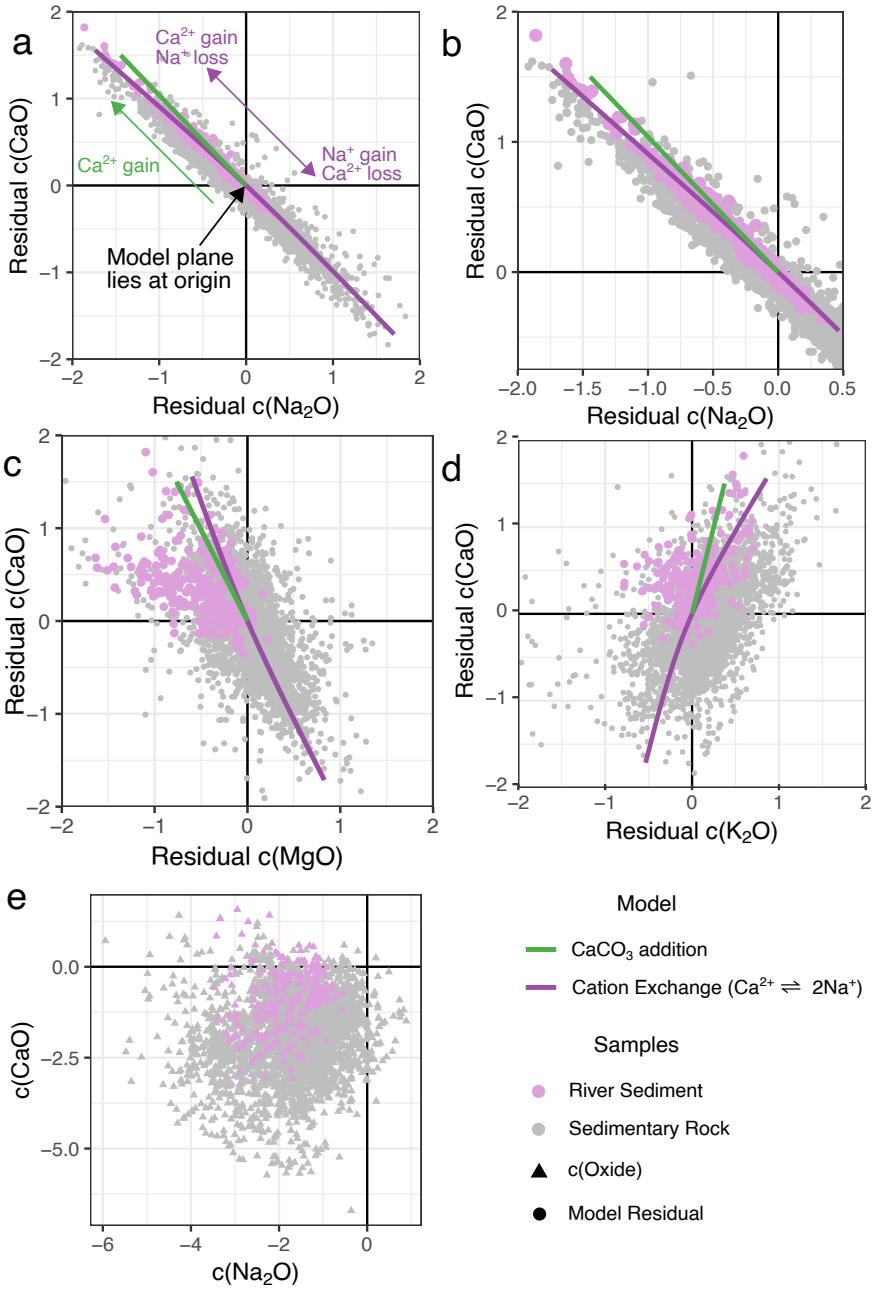

Figure 9. (a-d), Cross plots of *clr* residuals (grey points) for CaO, Na_2O, K_2O and MgO indicate systematic variation between residuals. The strong relationships between residuals is surprising given lack of clear relationship between the raw *clr* variables (e.g., Figure 9e). These residual relationships are compared to the modelled effect of calcite addition and cation exchange (green and purple lines respectively). First we consider a sediment which lies on the model plane. To model calcite addition we systematically vary the amount of Ca^{2+} in compositions. For cation exchange, Ca^{2+} and Na^{2+} were exchanged in molar quantities according to a 1:2 stoichiometry. The residuals of these new modified compositions are then calculated. The cation exchange trend closely fits the observed residuals for both positive and negative c(CaO) residuals. The modelled trends are independent of the initial composition of the sediment. Figure 9b is a close-up of Figure 9a

other components. The modelled effect of calcite addition on the residuals is shown in Figure 9. The modelled calcite addition trend is close to the observed trends in both river sediments and sedimentary rocks for positive c(CaO). However, because it is meaningless to consider a negative amount of calcite, it is impossible to generate the observed negative c(CaO) residuals for the sedimentary rocks and some river sediments.

An alternative process is cation exchange. Cations adsorbed to the surface of clays exchange with those in solution to maintain equilibrium with the surrounding fluid. Such reactions are important components of the geochemical cycling of a number of elements [*Sayles and Mangelsdorf*, 1977; *Cerling et al.*, 1989]. In natural sediments these reactions primarily occur when a fluvial sediment is deposited in seawater. Due to the sudden change in salinity and solute chemistry, clay-bound cations exchange with those in the seawater. The clays in the sediment are observed to exchange their Ca^{2+} for Na^{+}, K^{+} and Mg^{2+} from seawater [*Sayles and Mangelsdorf*, 1977; *Lupker et al.*, 2016]. As a result, a sedimentary rock deposited in a marine setting will have an excess of Na, Mg and K relative to the river sediment from which it derived.

Whilst all cations can exchange, the primary reaction observed in nature is an exchange of Na^{+} in solution for Ca^{2+} in clays according to the reaction:

$$Na_{2,\,clay} + Ca^{2+} \rightleftharpoons 2\,Na^{+} + Ca_{clay}$$

The modelled effect of this reaction upon the residuals closely matches the observed trends (Figure 9). Unlike carbonate addition, this can also explain negative c(CaO) residuals. This process also explains the distinct residual distributions of river sediments and sedimentary rocks. Figure 8 indicates that sedimentary rocks mostly have a positive residual for c(Na_2O) and c(MgO) and a negative residual for c(CaO). The river sediments have the opposite sense, with negative residuals for c(Na_2O) and c(MgO) and positive residual for c(CaO). These complementary residual distributions are consistent with the direction of exchange reactions observed in natural systems (e.g., *Lupker et al.* [2016]).

6.3 Effect of grain-size

Hydrodynamic sorting of sediments fractionates different mineral phases and changes the composition of a sediment (e.g., *Garzanti et al.* [2009]; *Bouchez et al.* [2011]). We want to know what effect sorting and grain-size has on a composition as described by our model. For example, sorting might alias $\hat{\mathbf{w}}$ or $\hat{\mathbf{p}}$, or contribute to out-of-plane misfit. We can constrain this effect using river sediments sampled at different depths in the water column [*Bouchez et al.*, 2011, 2012; *Lupker et al.*, 2012]. Samples collected from the same depth-profile are assumed to have the same provenance and to have been differentiated only by sorting.

Figure 10 shows the calculated weathering and provenance coefficients for samples collected in different depth profiles. ω is most strongly affected by sorting, with the largest observed difference of approximately 1 clr unit, around 15% of the total observed variability globally of ω. The coarse bedload of the sediment appears less weathered than the suspended load. ψ is weakly affected by sorting with a maximum intra-site variability (excluding bedload) of around 0.5 clr units. However, for ψ, the bedload shows no systematic deviation relative to the suspended load. Both of these variances are relatively small compared to the total observed variation in ψ and ω. We therefore conclude that sorting does affect composition, but that it can be considered as a relatively minor effect superimposed on top of the larger trends described by our model.

7 Application of model: Composition of the upper continental crust

We demonstrate the utility of our model (Equation 1) by describing the average composition of the UCC in terms of the processes from which it formed. It is proposed that the composition of UCC has been modified through time by chemical weathering (e.g., *Lee et al.*

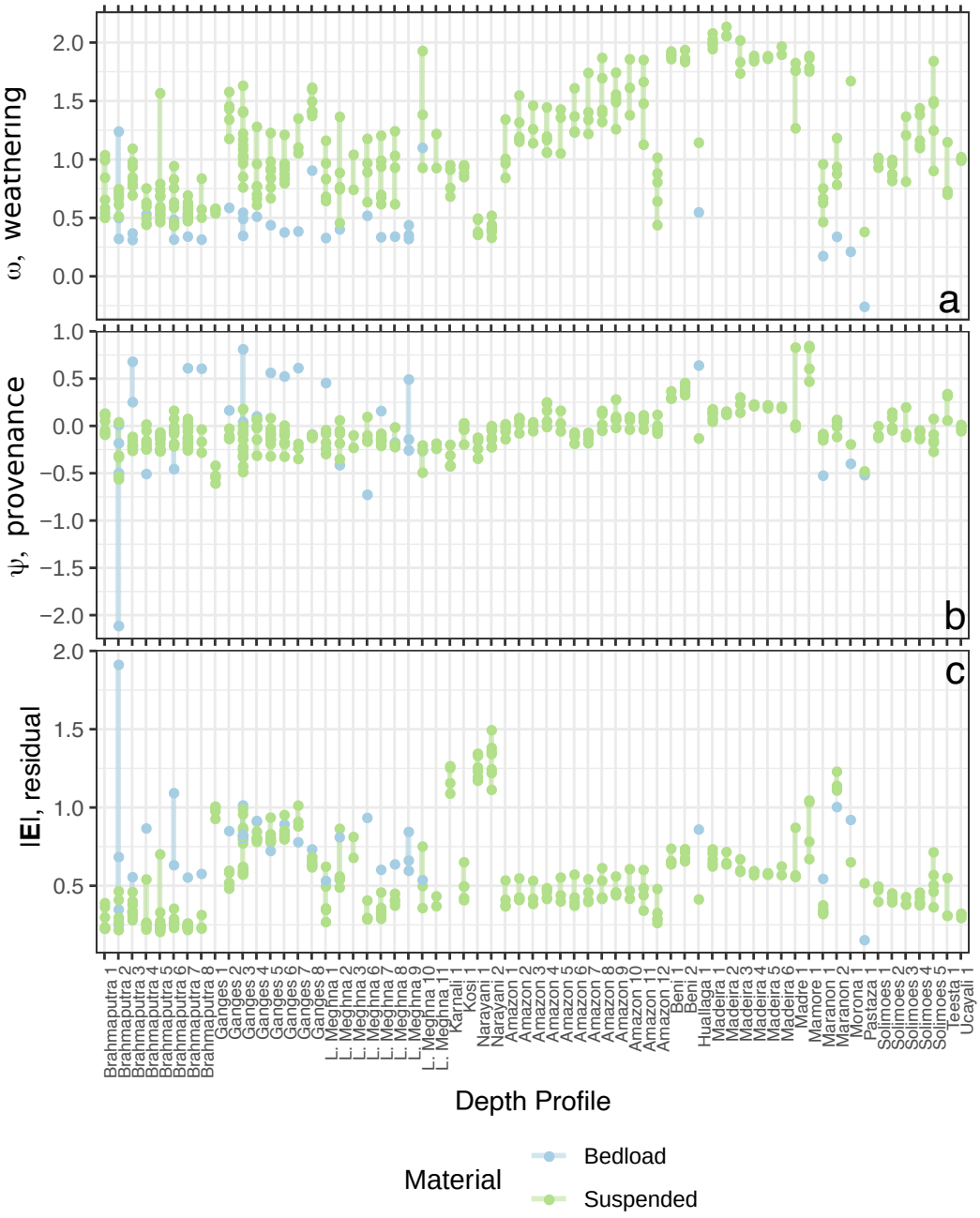

Figure 10. Figure indicating effect of sorting on the ω, ψ coefficients and residuals. Each vertical line corresponds to a suite of samples collected at the point on the a river on the same day, but at different vertical depths, referred to as a depth profile. Each point is a sediment sample from either the suspended load (green) or the bedload (blue). x-axis labels indicate the name of the river sampled. (a) Calculated ω values for depth-profiles. The suspended load mostly appears more weathered than the bedload. The maximum range within one site is approximately 1, at site "Brahmaputra 5". (b) same as Figure 10a but for ψ. Bedload can appear more mafic as well as more felsic than suspended load. Maximum range within suspended load is approximately 0.75 as site "Madre 6". (c) same as Figures 10a,b but for residual magnitude. Data from *Bouchez et al.* [2011, 2012]; *Lupker et al.* [2012]

[2008]). Chemical weathering enriches the weathering residue (i.e., sediments) in relatively insoluble elements, which may then be incorporated into the crust by accretion at subduction zones, or by incorporation into metamorphic rocks, such as S-type granites [*Rudnick*, 1995]. Recycling of weathered sediments back into the crust thus causes the continental crust to become progressively enriched in insoluble elements over time. This hypothesis is supported by independent isotopic proxies [*Simon and Lécuyer*, 2005; *Liu and Rudnick*, 2011]. Our model can in principle however, disentangle the effects of igneous and weathering processes using purely the major-element composition without using isotopic proxies.

If we want to interrogate whether UCC has been affected by weathering we need to define where pristine unweathered igneous rocks lie in ω, ψ space. The Crater Lake suite of igneous rocks likely lie approximately on this value but to buffer our value against any possi-

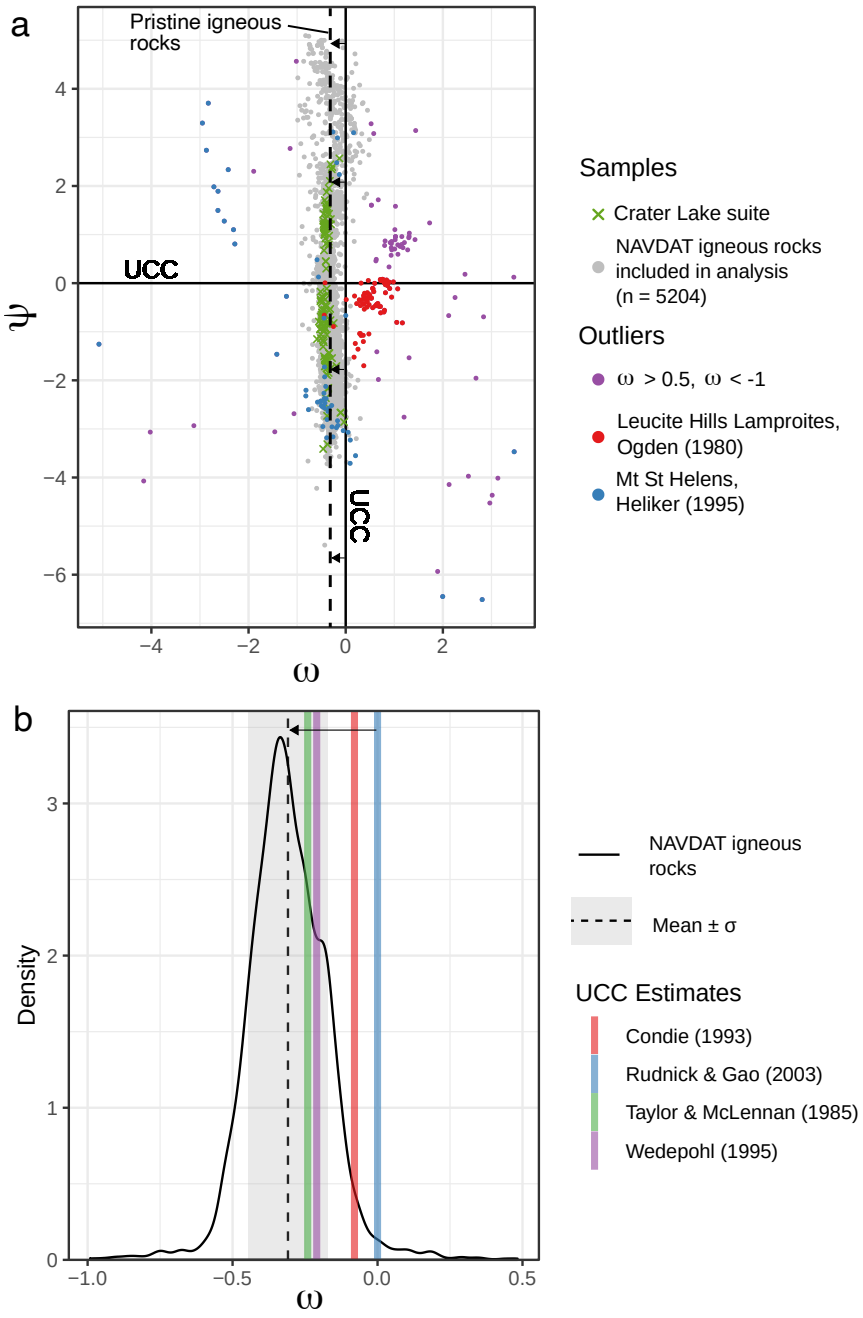

Figure 11. The composition of the upper continental crust, UCC, in terms of provenance, ψ, and weathering, ω, compared to juvenile igneous rocks. The UCC has a higher ω value than pristine igneous rocks, suggesting it has experienced weathering. (a) ω, ψ crossplot for 5204 igneous rocks from NAVDAT database (grey points). Black lines emphasise the composition of the UCC, which by definition lies at the origin. The igneous rocks lie on a vertical trend offset from UCC. Dashed line indicates mean ω value of igneous rocks, excluding anomalous samples (see below). Arrow indicates the offest between UCC and pristine igneous rocks. NAVDAT samples with $\omega > 0.5$ and $\omega < -1$, as well as from two studies with high numbers of anomalous samples [*Ogden*, 1979; *Heliker*, 1995] are indicated here but excluded from further analysis. (b) Black line = Kernel Density Estimate of the NAVDAT ω values, excluding anomalous samples indicated in Figure 11a. Vertical dashed line = mean NAVDAT ω value (-0.304), grey band = 1 σ confidence region for mean. Coloured vertical bands are the ω values for different estimates of UCC. Differences between these estimates are discussed in the body. All estimates lie offset positively, i.e., more weathered, than the NAVDAT mean. Arrow indicates the offest between the value of UCC we use and pristine igneous rocks.

ble local effects we gather a much larger database of igneous rocks. We analyse a dataset of North American igneous rocks extracted from the NAVDAT database (http://www.navdat.org/). We query for whole rock analyses of major-elements for recent (<1 Ma) plutonic and volcanic rocks from anywhere in North America. This yielded 5398 compositions once incomplete compositions were removed. The ω and ψ values for these values are shown in Figure 11. As expected these compositions lie on a linear trend of constant ω, consistent with the Crater Lake suite. There are a number of outliers to this trend, many of which come from two particular studies, which are treated as anomalous and excluded (Figure 11a). The distribution of the ω values for these samples is shown in Figure 11b, alongside the calculated ω values for different estimates of UCC [*Taylor*, 1985; *Condie*, 1993; *Wedepohl*, 1995; *Rudnick and Gao*, 2003].

The mean ω value for the pristine igneous rocks is -0.309 ± 0.137. This is less than the ω values for all the different estimates of UCC considered here (Figure 11b). All of these estimates of UCC therefore appear more weathered than the average pristine igneous rock. There are differences between the UCC estimates however. The estimates of *Taylor* [1985] and *Wedepohl* [1995] lie within one standard deviation of the mean pristine igneous rock. In contrast, the estimates of *Condie* [1993] and *Rudnick and Gao* [2003] have higher ω values, with the latter lying 2 standard deviations from the mean pristine igneous rock values.

The differences between the estimates partly reflect different methods in calculating the composition of UCC. *Rudnick and Gao* [2003] calculate UCC by averaging a large number of surface outcropping rock compositions, including sedimentary cover. *Condie* [1993] also includes sedimentary rocks in their calculation, but introduce a weighting to the average composition by areal outcrop of different rock-types. In contrast, *Taylor* [1985] and *Wedepohl* [1995] calculate their compositions of UCC based off of the same large-scale sampling survey of the Canadian shield. That these estimates appear less weathered than the others may reflect sampling of a smaller proportion of sedimentary rocks due to the geology of the Canadian shield [*Rudnick and Gao*, 2003]. We use the estimate of *Rudnick and Gao* [2003] as the canonical composition for UCC as it is calculated by averaging the largest number of samples from across different continents.

7.1 Quantification of mass loss due to weathering

Taking the estimate of *Rudnick and Gao* [2003] as the value of UCC we can estimate how much mass must have been removed from UCC by chemical weathering. We define a pristine precursor rock for UCC by projecting the UCC composition to the ω value defined by the pristine igneous rock trend. This gives a composition, $\mathbf{x}_0$, as shown in Table 4 along-

Table 4. Values used and produced in the calculation to estimate the amount of mass lost of each element from the upper continental crust due to weathering. $\mathbf{x_1}$ is the present day composition of UCC. $\mathbf{x_0}$ is the predicted pristine precursor to the upper crust calculated using the model. $\mathbf{f}$ is the fractional mass loss of each estimate assuming Al_2O_3 immobility. $\mathbf{M}_0$ is the estimated mass of each element of the unweathered continental crust. $\Delta\mathbf{M}$ is the calculated mass loss of each element given both in oxide and elemental form. Details of the calculation are given in the body text.

	SiO_2	Al_2O_3	Fe_2O_3	MgO	Na_2O	CaO	K_2O
$\mathbf{x_1}$	66.8	15.4	5.61	2.49	3.28	3.60	2.81
$\mathbf{x_0}$	65.7	14.4	5.70	2.57	4.11	4.67	2.82
$\mathbf{f}$	-0.0494	0	-0.0790	-0.0936	-0.254	-0.279	-0.0675
$\mathbf{M}_0$ / 10^{19} kg	383	84.2	33.3	15.0	24.0	27.2	16.4
$\Delta\mathbf{M}$ / 10^{19} kg (oxide)	-18.9	0	-2.62	-1.40	-6.09	-7.59	-1.11
$\Delta\mathbf{M}$ / 10^{19} kg (elemental)	-8.85	0	-1.84	-0.844	-4.52	-5.43	-0.921

side the observed present day UCC composition, $\mathbf{x}_1$. This composition suggests a granitic (SiO_2 = 65.7 %) igneous precursor to the present UCC, which is not a primary mantle melt. Therefore, we assume that a process of igneous differentiation acted upon a primary mantle melt, to create a granitic precursor, prior to being weathered to its present day composition.

The compositions of the UCC and its pristine precursor only contain information about the relative mass of its components. To calculate the absolute mass difference between the two compositions we need to identify an element to act as a reference point. Aluminium is typically not mobilised during weathering remaining almost totally in the weathering restite, so we make the assumption that the total mass of Al_2O_3 is constant. Making this assumption, for an observed composition, $\mathbf{x_1}$, we can calculate the fractional mass change of each element, $\mathbf{f}$, relative to the initial composition $\mathbf{x_0}$ as follows

$$f_i = \frac{\Delta M_i}{M_{i,0}} = \frac{x_{i,1}}{x_{i,0}} \cdot \frac{x_{\mathrm{Al_2O_3},0}}{x_{\mathrm{Al_2O_3},1}} - 1, \tag{9}$$

where $\mathbf{M}_0$ is a vector of the initial mass of each element, i, and $\mathbf{\Delta M}$ is a vector of the absolute mass change of each element. The calculated values of $\mathbf{f}$ for the upper crust are shown in Table 4.

To calculate the absolute amount of mass lost from the crust due to weathering, we require an estimate of the initial mass of the crust prior to weathering. To calculate this value we multiply estimates of the volume of the upper crust by an appropriately chosen density. The initial composition of the precursor rock, x_0, is felsic so we assume an initial density of 2700 kg m^{-3}. The volume of the total continental crust is given by *Cawood et al.* [2013] to be 7.2×10^{18} m^3 of which UCC makes up the upper 30% of the thickness. This means that UCC has a volume $\sim$ 0.3 times that of the total continental crustal volume, giving 2.16×10^{18} m^3. Using a density of 2700 kg m^{-3}, we estimate that UCC had an initial mass of 5.83×10^{21} kg, assuming a constant crustal volume (i.e., isovolumetric weathering). The initial mass of each element can be calculated by multiplying this value by the composition $\mathbf{x_0}$, shown in Table 4. The absolute change in mass for each element, ΔM_i, can thus be calculated by

$$\Delta M_i = f_i \cdot M_{i,0}. \tag{10}$$

The calculated mass loss for each oxide is shown in Table 4, also displayed converted to elemental mass losses.

This estimate makes the assumption of negligible mass contribution of other minor elements. Given that the major-elements, by definition, make up the bulk composition of a sediment this assumption is probably appropriate. In addition this estimate only considers

the silicate portion of the UCC. Much of the calcium, and some of the magnesium, lost from the silicate crust by weathering is reincorporated as carbonate sediments which are not considered in the bulk composition of UCC considered here.

7.2 Implications for the fate of crustal sediments

We have calculated the mass of each element lost by weathering required to evolve a juvenile felsic igneous protolith to the modern UCC composition. Now we compare these values to the present day mass fluxes derived from silicate weathering shown in Table 5 (data for Fe and Al was not available). We can use these two values to calculate a "weathering age" of the UCC for each element, which is the time it takes, at present weathering rates, to modify the UCC composition to its present state. This age is calculated by dividing the mass loss for each element by the dissolved load flux for that element. However, when these values are calculated, they are considerably less than the expected age of the crust. For example, *Taylor* [1985] estimate that most of the continental crust formed by 2.5 Ga, but the "weathering ages" of the UCC range from ~ 800 Ma for Na to ~ 120 Ma for Mg. Ca, Si and K return ages of ~ 550, ~ 480 and ~ 200 Ma respectively.

The discrepancy between these ages of $O(100)$ Ma) and the model crustal age of 2.5 Ga could be a result of the assumption in the calculation that all of the solid weathering restite is retained on the crust during weathering. If the restite, however, is transported with the dissolved weathering products off the continents the net composition of the crust does not change. Should this be the case the "weathering ages" calculated above will be an underestimate, because this makes weathering less efficient in evolving crustal composition than the dissolved elemental fluxes alone imply. Given that solid weathering products, "restite", are transported to ocean basins by rivers and glaciers this likely explains why these age estimates do not agree with externally calibrated ages of the crust. This hypothesis is supported by the fact that most sediments stored on the continental crust are Phanerozoic in age consistent with the $O(100)$ Ma) weathering ages we derive above [*Peters and Husson*, 2017]. The next logical step is to estimate the amount of this restite which has not been incorporated into the crust.

The mass of dissolved material required to modify the present day composition of the UCC (Table 4) can be considered "balanced" by a restite retained on the continents and contributing to its present composition. The amount of "unbalanced" dissolved weathering product is therefore the difference between these balanced values, and the total amount of dissolved weathering product produced since the formation of the crust at ~ 2.5 Ga. An estimate of the time integrated dissolved product for each element is shown in Table 5, calculated by simply extrapolating present day silicate weathering rates over 2.5 Ga.

This unbalanced dissolved weathering product can be used to estimate the amount of unbalanced solid weathering restite, by assuming a characteristic ratio of dissolved to solid products produced during silicate weathering. In this instance we calculate the ratios using the average amount of mass of each element carried in suspension relative to solution in rivers globally, using values from *Berner* [2012]. These ratios are used to calculate the total amount of restite (i.e., terrigenous sediments) in excess of that restite which has been incorporated into the upper crust, as shown in Table 5. These can be used to estimate the total mass of the restite, if we assume that it has the typical composition of a sedimentary rock. For this typical composition we use the arithmetic mean of the compositions in our sedimentary rock dataset. The total amount of mass is found by dividing the modelled mass of each restite element by the proportion within a sediment. All of the elements independently give similar values, with an average value of $3.68 \pm 2.50 \times 10^{22}$ kg.

Table 5. Values used to estimate solid weathering restite transported off the upper continental crust. The total weathering mass loss is the amount of mass removed from crust in solution at present weathering rates using a model crustal age of 2.5 Ga [*Taylor*, 1985]. The "unbalanced" dissolved mass is the difference between the total mass loss and the mass loss that can be explained by the weathered present day UCC composition (Table 4). Assuming a characteristic ratio for how much of each element is produced in solution relative to solid restite we can thus calculate the amount of each element that has been net transported off the upper continental crust as weathering restite, i.e., sediments. Using the average composition of the sedimentary rocks in our dataset we can turn each of these estimates into a total mass of the "missing" sediment. All the estimates agree within an order of magnitude giving an average value of $3.68 \pm 2.50 \times 10^{22}$ kg

	Si	Mg	Na	Ca	K
Silicate weathering flux (dissolved)[1] / 10^{10} kg/yr	18.3	7.27	5.65	9.87	4.59
Time integrated weathering mass loss (dissolved) / 10^{20} kg	4.56	1.82	1.41	2.47	1.15
Unbalanced weathering product (dissolved) / 10^{20} kg	**3.68**	**1.73**	**0.962**	**1.92**	**1.05**
Silicate weathering solid:dissolved ratio[2]	20.9	2.60	1.89	3.94	5.54
Element-wise unbalanced weathering product (solid) / 10^{20} kg	**76.9**	**4.51**	**1.82**	**7.59**	**5.84**
Average sedimentary rock composition[3] / wt%	29.2	1.33	0.873	0.941	2.62
Total unbalanced weathering product (solid) / 10^{22} kg	**2.64**	**3.39**	**2.08**	**8.07**	**2.23**

[1] Values calculated from *Berner* [2012] derived from global river compilations, correcting for human influence;

[2] Calculated from *Berner* [2012] using the average ratio of mass transported in solution (silicate derived fraction) relative to suspended sediment in rivers globally. This assumes steady state weathering;

[3] Calculated using the arithmetic mean of the raw wt% elemental composition for the sedimentary rock dataset.

7.3 Implications of UCC composition for crustal recycling

Using the composition of UCC we have estimated the size of a reservoir of weathering restite that has been produced by chemical weathering over the age of the crust but has not been incorporated into the upper crust itself. This still leaves the location of this sedimentary reservoir unresolved. One possibility is that the sediment has simply been deposited in the ocean basins. The volume of sediment deposited on continental margins has been estimated by *Straume et al.* [2019] to be 1.43×10^{17} m^3. Assuming a density of 2500 kgm^{-3} this corresponds to a mass of 3.58×10^{20} kg, which is only 1.02 % of our estimate of the size of the reservoir. We thus discount the ocean basins as a potential long-term sink. Furthermore, the oldest oceanic crust is roughly 200 Ma in age, precluding it as a long-term sink for sediments in the context of the 2.5 Ga age of the continental crust. Consequently there is 10^{22} kg of sediment that has neither been incorporated into the upper continental crust, nor at present stored in the ocean basins. We suggest then that the sediment has likely been removed from the Earth's surface via subduction zones.

For such a volume of sediment to be subducted is striking, as the mass we calculate is approximately six times our estimate of the present day mass of the upper crust (Table 4). This would suggest that since its formation 2.5 Ga, the upper crust has been recycled multiple times, with the solid product subducted into the mantle (or at least isolated from the upper crust, for example incorporated into the lower crust). How does this value compare to other estimates of crust-to-mantle recycling rates? Assuming the sediment reservoir is recycled uniformly over 2.5 Ga, this gives a recycling rate of $1.47 \pm 1.00 \times 10^{13}$ kg yr^{-1}. This estimate is slightly higher than but, within error, comparable to other estimates of crust-to-mantle recycling rates which range from < 0.11 to 0.84×10^{13} kg yr^{-1} [*McLennan*, 1988].

Is it possible to subduct sedimentary material at this rate? Assuming that the subducted ocean crust has a plausible thickness of 1 km of crustal derived sediments deposited on it, this requires an oceanic crust subduction rate of 5.88 km^2 yr^{-1}. *Bird* [2003] estimate that present day subduction zones are 6×10^5 km in length. Assuming this value is approximately stable through time, to subduct the material requires a plate convergence rate of 9.8 cm yr^{-1}. This convergence rate is comparable to average subduction velocities calculated from plate and geodynamic models (e.g., *Behr and Becker* [2018]). This simple calculation shows that the mantle could be the repository for our sediment reservoir.

It is important to consider alternative explanations, especially explanations for why our estimate of crust-mantle recycling rate is larger than previous estimates. One possibility is that the calculated composition of UCC in *Rudnick and Gao* [2003] is not representative and in reality the UCC has incorporated more restite, but it is not represented by the composition at the surface. This could occur if the restite is preferentially incorporated below the surface. Given that sediments however are generally deposited in sedimentary basins at the surface of the crust, this seems unlikely.

Another possibility is that the value of UCC we use is not representative of the upper crust. In other words the restite is incorporated heterogeneously laterally, and has so far not been sampled for estimates of the average composition of UCC. Such large scale heterogeneity is potentially conceivable as prior estimates of UCC composition, which sampled smaller areas of the surface, are observably different to the *Rudnick and Gao* [2003] estimate we use that considers more data (Figure 11b). For this effect to explain the totality of the missing reservoir, the unsampled portion of UCC would have to contain the total amount of restite we consider "missing", which is implausible. However it is possible that our estimate of recycling rate could be be brought closer to alternate estimates, should future estimates of UCC composition are found to be more intensely weathered than *Rudnick and Gao* [2003]'s estimate.

A further possibility is that present day weathering rates cannot be extrapolated over 2.5 Ga and that they were lower in the past. Such a possibility is difficult to rule out because

quantitative constraints on weathering rates are lacking in deep time. However, one constraint on this comes from weathering's role as a long term carbon sink. To maintain a stable climate over 2.5 Ga, the chemical weathering rate must broadly be set by the rate of mantle CO_2 degassing [*Broecker and Langmuir*, 1985]. Consequently, unless CO_2 degassing rates were much lower in the past, it is difficult to conceive how the weathering rate also was at a lower level for sustained periods of time. Consequently, whilst this is difficult to conclusively rule out, on the basis of a stable climate we consider that a sustained lower weathering rate is unlikely.

Thus, whilst we consider the potential limitations of the data used, if one assumes that the calculated composition of UCC is correct, and also that global silicate weathering rates have remained mostly constant since 2.5 Ga, the conclusion is that there is an amount of sediment, equal in mass to six times the present day upper crust, that has likely been removed from the crust by subduction.

8 Discussion

First, we discuss why the apparently complex set of processes that control the composition of a sediment can be simplified to a linear 2D model. Secondly, we review the other approaches to analysing sedimentary geochemical compositions and discuss some advantages of the approach we propose.

8.1 Simple 2D provenance and weathering formulations

A straight line fit in clr space appears to match the weathering and provenance trends. A straight line in clr space is a manifestation of exponential growth/decay of absolute masses, which is intuitive given that the clr transformation is logarithmic [*Pawlowsky-Glahn*, 2015b]. Therefore, the straight line fits to weathering and provenance indicates that during these processes the absolute mass of each oxide decays exponentially relative to each other for unit changes of ω and ψ.

Sediments derive from a range of different rocks which can broadly be divided into primary igneous rocks, recycled sedimentary rocks and metamorphic rocks formed by melting of pre-existing crustal rocks. Each of these groups show internal compositional variability. How can this complexity be reconciled with the observation that assuming a one-dimensional provenance vector successfully explains much of the compositional variation in sediments?

First, we have shown primary igneous variation to be well approximated by a single vector (Figure 11a). This suggests distinctions such as alkaline/subalkaline are minor variations superimposed on the larger igneous evolution trend. Secondly, sedimentary recycling can be considered in our framework in terms of linear addition. Consider a sediment that lies on the 2D plane defined by $\hat{\mathbf{w}}$ and $\hat{\mathbf{p}}$. If this sediment is recycled, any derived sediment will also lie on this plane, possibly translated along the $\hat{\mathbf{w}}$ vector. Thus, it is not possible (from major-elements alone) to distinguish a recycled sediment from a 'primary' sediment. This inability to identify recycled sediments is not a limitation with our approach specifically, but rather a larger problem with using purely elemental geochemistry. Finally, metamorphic processes occurring in a closed system will not affect the protolith's major-element chemistry, and are therefore compatible with our assumptions. However, if the metamorphosing sediment melts and this melt was extracted (e.g., to produce an S-type granite) this could cause a change in major-element chemistry not accounted for in our model. That the model is still successful despite such processes may be explained firstly by partial melting during prograde metamoprhism evolving compositionally parallel to the primary igneous vector, $\hat{\mathbf{p}}$. Secondlym it could indicate partial melting is not ubiquitous enough to generate significant misfit when considering geographically extensive datasets. Finally, it could be that metamorphic

partial melts remain close to their source rocks on the regional scale of sedimentary routing systems.

8.2 The effect of cation exchange and sorting on composition

Considered in terms of Equation 1, weathering and provenance account for the majority (59.4%) of sedimentary rock compositional variability. Factors such as cation exchange and sorting may locally modify compositions but only superimposed on the larger scale trend set by weathering and provenance.

The model residuals correspond to compositional variation caused by any other process which is not weathering or provenance, including analytical noise. Cation exchange, particularly Na^+ for Ca^{2+} has a siginificant control on composition. Fluvial sediments tend to be enriched in CaO because of this process. In contrast, sedimentary rocks that may have experienced contact with sodium rich seawater are often enriched in Na_2O. However, in the direction of CaO enrichment this is difficult to distinguish from carbonate addition in residual space. Other reactions will act to modify a composition, however the trend defined by Na-Ca exchange appears to define the most significant variation in residuals.

8.3 A comparison to other methods of sedimentary geochemical analysis

Compositions only contain information about the relative values of their components, as opposed to absolute values [*Aitchison*, 1982]. Consequently, a common approach to analyse sedimentary compositions, and geochemical data in general, is to use indices derived from elemental ratios as proxies for specific processes. For example, the Chemical Index of Alteration (CIA) and Chemical Index of Weathering (CIW) [*Nesbitt and Young*, 1982; *Harnois*, 1988] as proxies for weathering, the Al/Si ratio as a proxy for sorting [*Bouchez et al.*, 2011] and the Ni/Co and Cr/Zn ratios as proxies for igneous evolution [*Tang et al.*, 2016]. Comparing the ω value that we derive to the other weathering proxies of CIA and CIW (Figure 12a,b) shows a good correspondence, as expected if all these indices reliably track weathering (Figure 12a,b). Our index in design is most similar to the W index of *Ohta and Arai* [2007], who use PCA on a suite of soil compositions to define weathering and provenance indices which have a number of advantages over elemental ratios. However, *Ohta and Arai* [2007] directly interpret the first and second principal components of their dataset as weathering and provenance vectors. Whilst this might be a useful approximation, it is inappropriate if the vectors are not orthogonal, which our analysis indicates to be the case.

Ratio derived proxies are intuitive, simple to calculate and examples such as the CIA have been extensively and successfully used to extract meaningful information from compositions in a very large number of studies. However, there are some limitations to using elemental ratios and their derived proxies, which the approach we articulate in this study does not suffer from.

A first limitation is that by simplifying an entire composition to a ratio involving only a small number of constituent components, any relevant information contained within the other components is lost. In general, elements chosen to be used in a ratio are those which exhibit contrasting behaviours in response to a particular process, such that their ratio varies strongly upon action of that process. For example, Al, as a major constituent of clay minerals, is concentrated in fine sedimentary fractions, whereas Si, concentrated in the most refractory silicate minerals such as quartz, is concentrated in the coarse fraction; the Al/Si ratio is thus sensitive to sorting and grain-size through both its numerator and denominator. However, whilst it may be true that two elements are particularly sensitive to a given process, this does not mean that all other components of a composition are unaffected by that process. The approach we present, by contrast, is rooted in multivariate statistics and can extract all the information relating to weathering and provenance contained within the 7 component system we choose.

Table 6. Oxides wt% ratios which are useful proxies

Ratio	Process
$\ln(Al_2O_3/Na_2O)$	ω, Weathering
$\ln(K_2O/MgO)$	ψ, Provenance
$\ln(Na_2O/CaO)$	Residual c(Na_2O), Cation exchange

Secondly, used on face value, ratio derived proxies lack predictive power and by extension lack information about misfit between the process the ratio is nominally sensitive to and the dataset is being applied to. For example, from a particular composition the CIA may inform us of how intensely a sediment has been weathered but the CIA alone cannot be used to reconstruct the total composition, nor constrain how the composition might change if weathering were to act further. An important corollary of lacking predictive power is that a ratio-derived index alone cannot indicate whether it is being appropriately applied in each instance. The assumption of using a ratio derived proxy is that the chosen ratio has been affected exclusively by the process for which it is a proxy. If however it has been affected by additional processes that also affect the ratio, the derived proxy alone can potentially not reveal this. This is a challenging problem in instances where an initial primary signal may be being overwritten by diagenetic processes. The model we propose here however does have predictive power about the effect of weathering and provenance on compositions. Consequently, our model has a misfit term which quantifies the extent to which processes not considered within the model may have affected it. The importance of this misfit term was demonstrated by its ability to identify the possible role of a secondary process, namely cation exchange, in controlling sediment composition, on top of weathering and provenance.

Finally, when ratio derived proxies have the same denominator, they can be subject to the problem of spurious correlation of ratios, an issue noted for over 100 years [*Pearson*, 1897]. For example, consider the ratios Ca/Si and Fe/Si, plausibly devised so as to investigate the intensity of weathering and provenance respectively on a sediment. However, despite the independent nature of the processes being investigated through these ratios, their construction, with Si common to both denominators, will ensure that a spurious correlation emerges. This effect could confound attempts to pick apart multiple processes acting upon a sediment. By contrast, the indices we derive in this study, ω and ψ, are independent of each other and therefore not subject to this effect.

Whilst we argue that these limitations ought to be heeded, we appreciate the convenience and ease-of-use which geochemical ratios offer as data exploratory tools. We have therefore identified three log-ratios of wt% data which are closely linearly related to weathering, provenance, and cation exchange respectively (Figure 12c-f, Table 6). These are easy to calculate and can act as approximate 'rules-of-thumb' indicators and data exploratory tools of what the ω and ψ coefficients might be. However, use of these ratios requires careful consideration of the limitations of ratio proxies outlined above.

9 Conclusions

Weathering and provenance are the dominant controls on the major-element composition of sediments. We have developed a model that describes a sediment composition in terms of these processes. When applied to fine-grained sediments, the model is successful in explaining the majority of observed compositional variation in all types of sediment. Deviations from model predictions indicate what important secondary processes may have affected a sediment's composition. Inspection of these deviations suggest that cation exchange of sodium and calcium is an important process in determining sediment composition. The model can be used to calculate the composition of a sediment's protolith and the intensity of weathering it has experienced.

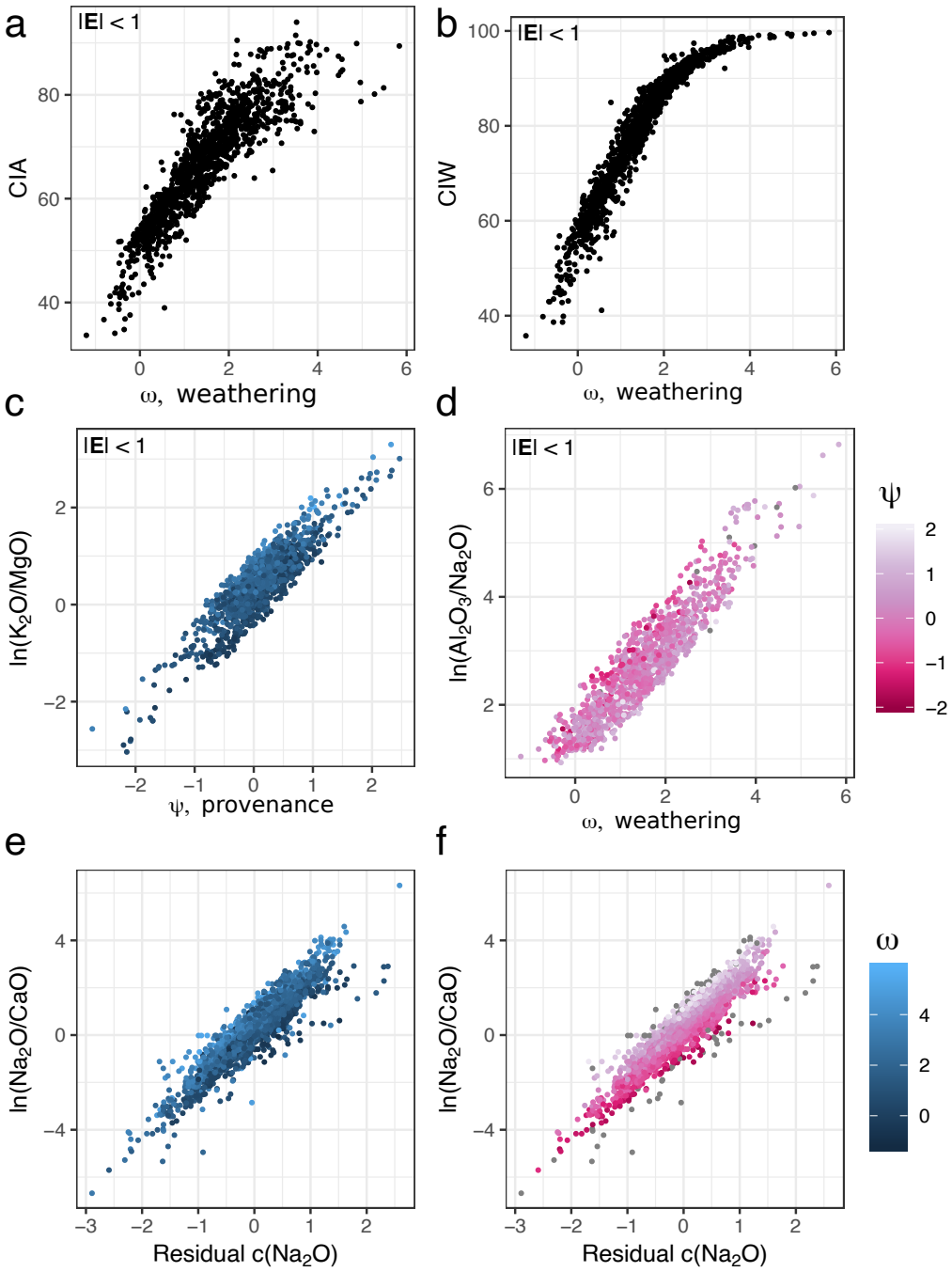

Figure 12. Comparison of ω to the Chemical Index of Alteration (CIA) (a) and Chemical Index of Weathering (CIW) (b) shows that all are strongly related, but the CIW saturates at higher ω values.(c) indicates that $\ln K_2O/MgO$ is a good proxy for ψ and is weakly affected by weathering. (d) indicates that $\ln Al_2O_3/Na_2O$ is a good proxy for ω and is weakly affected by provenance. (e) & (f) indicate that $\ln Na_2O/CaO$ is a good proxy for diagenesis and is weakly affected by both weathering and provenance. Figures 12a-d only show samples with residual magnitude < 1.

The utility of our approach is demonstrated by showing that the composition of the upper continental crust has been modified by weathering, relative to a pristine igneous precursor. We quantify the mass of each element which has been removed by weathering to sufficiently modify the composition of UCC to its present state. When compared to modern weathering rates, we conclude that significant amounts of weathering restite, i.e., sediment, has not been incorporated into the upper continental crust. The amount of this sediment, $3.68 \pm 2.50 \times 10^{22}$ kg, is too large to be stored in the ocean basins and so we conclude it is likely subducted into the mantle. This is equal to six times the present mass of the upper continental crust suggesting the crust has experience multiple complete recycling events.

Acknowledgments

Code and compiled data can be found at github.com/AlexLipp/weathering-and-provenance and is archived at the point of submission at doi.org/10.5281/zenodo.3483063. AGL is supported by a NERC studentship with a CASE award from CASP. FS is supported by a NERC studentship with a CASE award from Schlumberger Cambridge Research. We thank Michael Flowerdew, Victoria Fernandes, and Jennifer Quye-Sawyer for their input.

References

Aitchison, J. (1982), The Statistical Analysis of Compositional Data, *Journal of the Royal Statistical Society. Series B (Methodological)*, *44*(2), 139–177.

Aitchison, J. (1983), Principal component analysis of compositional data, *Biometrika*, *70*(1), 57–65, doi:10.1093/biomet/70.1.57.

Aitchison, J. (1986), *The statistical analysis of compositional data*, Chapman and Hall.

Aitchison, J., and J. J. Egozcue (2005), Compositional Data Analysis: Where Are We and Where Should We Be Heading?, *Mathematical Geology*, *37*(7), 829–850, doi:10.1007/s11004-005-7383-7.

Behr, W. M., and T. W. Becker (2018), Sediment control on subduction plate speeds, *Earth and Planetary Science Letters*, *502*, 166–173, doi:10.1016/j.epsl.2018.08.057.

Berner, E. K. (2012), Chapter 5. Rivers, in *Global environment: water, air, and geochemical cycles*, 2nd ed. ed., pp. 185–257, Princeton University Press, Princeton, N.J. ; Oxford.

Bird, P. (2003), An updated digital model of plate boundaries, *Geochemistry, Geophysics, Geosystems*, *4*(3), doi:10.1029/2001GC000252.

Bloemsma, M. R., M. Zabel, J. B. W. Stuut, R. Tjallingii, J. A. Collins, and G. J. Weltje (2012), Modelling the joint variability of grain size and chemical composition in sediments, *Sedimentary Geology*, *280*, 135–148, doi:10.1016/j.sedgeo.2012.04.009.

Bouchez, J., J. Gaillardet, C. France-Lanord, L. Maurice, and P. Dutra-Maia (2011), Grain size control of river suspended sediment geochemistry: Clues from Amazon River depth profiles, *Geochemistry, Geophysics, Geosystems*, *12*(3), doi:10.1029/2010GC003380.

Bouchez, J., J. Gaillardet, M. Lupker, P. Louvat, C. France-Lanord, L. Maurice, E. Armijos, and J.-S. Moquet (2012), Floodplains of large rivers: Weathering reactors or simple silos?, *Chemical Geology*, *332-333*, 166–184, doi:10.1016/j.chemgeo.2012.09.032.

Broecker, W. S., and C. H. Langmuir (1985), Making it comfortable, in *How to build a habitable planet*, pp. 298–386, Princeton University Press.

Buccianti, A. (2013), Is compositional data analysis a way to see beyond the illusion?, *Computers & Geosciences*, *50*, 165–173, doi:10.1016/j.cageo.2012.06.012.

Cawood, P., C. Hawkesworth, and B. Dhuime (2013), The continental record and the generation of continental crust, *Geological Society of America Bulletin*, *125*(1-2), 14–32, doi:10.1130/B30722.1.

Cerling, T. E., B. L. Pederson, and K. L. V. Damm (1989), Sodium-calcium ion exchange in the weathering of shales: Implications for global weathering budgets, *Geology*, *17*(6), 552–554, doi:10.1130/0091-7613(1989)017<0552:SCIEIT>2.3.CO;2.

Condie, K. C. (1993), Chemical composition and evolution of the upper continental crust: Contrasting results from surface samples and shales, *Chemical Geology*, *104*(1), 1–37, doi:10.1016/0009-2541(93)90140-E.

Cullers, R. L., T. Barrett, R. Carlson, and B. Robinson (1987), Rare-earth element and mineralogic changes in Holocene soil and stream sediment: A case study in the Wet Mountains, Colorado, U.S.A., *Chemical Geology*, *63*(3), 275–297, doi:10.1016/0009-2541(87)90167-7.

Fedo, C. M., H. W. Nesbitt, and G. M. Young (1995), Unraveling the effects of potassium metasomatism in sedimentary rocks and paleosols, with implications for paleoweathering conditions and provenance, *Geology*, *23*(10), 921–924, doi:10.1130/0091-7613(1995)023<0921:UTEOPM>2.3.CO;2.

Gaillardet, J., B. Dupré, and C. J. Allègre (1999), Geochemistry of large river suspended sediments: silicate weathering or recycling tracer?, *Geochimica et Cosmochimica Acta*, *63*(23), 4037–4051, doi:10.1016/S0016-7037(99)00307-5.

Garzanti, E., S. Andò, and G. Vezzoli (2009), Grain-size dependence of sediment composition and environmental bias in provenance studies, *Earth and Planetary Science Letters*, *277*(3), 422–432, doi:10.1016/j.epsl.2008.11.007.

Harnois, L. (1988), The CIW index: A new chemical index of weathering, *Sedimentary Geology*, *55*(3), 319–322, doi:10.1016/0037-0738(88)90137-6.

Heliker, C. (1995), Inclusions in Mount St. Helens dacite erupted from 1980 through 1983, *Journal of Volcanology and Geothermal Research*, *66*(1), 115–135, doi:10.1016/0377-0273(94)00074-Q.

Lee, C.-T. A., D. M. Morton, M. G. Little, R. Kistler, U. N. Horodyskyj, W. P. Leeman, and A. Agranier (2008), Regulating continent growth and composition by chemical weathering, *Proceedings of the National Academy of Sciences*, *105*(13), 4981–4986, doi:10.1073/pnas.0711143105.

Liu, X.-M., and R. L. Rudnick (2011), Constraints on continental crustal mass loss via chemical weathering using lithium and its isotopes, *Proceedings of the National Academy of Sciences*, *108*(52), 20,873–20,880, doi:10.1073/pnas.1115671108.

Lupker, M., C. France-Lanord, V. Galy, J. Lavé, J. Gaillardet, A. P. Gajurel, C. Guilmette, M. Rahman, S. K. Singh, and R. Sinha (2012), Predominant floodplain over mountain weathering of Himalayan sediments (Ganga basin), *Geochimica et Cosmochimica Acta*, *84*, 410–432, doi:10.1016/j.gca.2012.02.001.

Lupker, M., C. France-Lanord, and B. Lartiges (2016), Impact of sediment-seawater cation exchange on Himalayan chemical weathering fluxes, *Earth Surface Dynamics Discussions*, pp. 1–15, doi:10.5194/esurf-2016-26.

Martin, J.-M., and M. Meybeck (1979), Elemental mass-balance of material carried by major world rivers, *Marine Chemistry*, *7*(3), 173–206, doi:10.1016/0304-4203(79)90039-2.

Martín-Fernández, J. A., C. Barceló-Vidal, and V. Pawlowsky-Glahn (2003), Dealing with Zeros and Missing Values in Compositional Data Sets Using Nonparametric Imputation, *Mathematical Geology*, *35*(3), 253–278, doi:10.1023/A:1023866030544.

McLennan, S. M. (1988), Recycling of the continental crust, *Pure and Applied Geophysics PAGEOPH*, *128*(3-4), 683–724, doi:10.1007/BF00874553.

Nesbitt, H. W. (1979), Mobility and fractionation of rare earth elements during weathering of a granodiorite, *Nature*, *279*(5710), 206, doi:10.1038/279206a0.

Nesbitt, H. W., and G. Markovics (1997), Weathering of granodioritic crust, long-term storage of elements in weathering profiles, and petrogenesis of siliciclastic sediments, *Geochimica et Cosmochimica Acta*, *61*(8), 1653–1670, doi:10.1016/S0016-7037(97)00031-8.

Nesbitt, H. W., and G. M. Young (1982), Early Proterozoic climates and plate motions inferred from major element chemistry of lutites, *Nature*, *299*(5885), 715, doi:10.1038/299715a0.

Nesbitt, H. W., and G. M. Young (1989), Formation and Diagenesis of Weathering Profiles, *The Journal of Geology*, *97*(2), 129–147, doi:10.1086/629290.

Nesbitt, H. W., G. Markovics, and R. C. price (1980), Chemical processes affecting alkalis and alkaline earths during continental weathering, *Geochimica et Cosmochimica Acta*, *44*(11), 1659–1666, doi:10.1016/0016-7037(80)90218-5.

Nesbitt, H. W., G. M. Young, S. M. McLennan, and R. R. Keays (1996), Effects of Chemical Weathering and Sorting on the Petrogenesis of Siliciclastic Sediments, with Implications for Provenance Studies, *Journal of Geology*, *104*, 525–542, doi:10.1086/629850.

Ogden, P. R. (1979), The geology, major element geochemistry, and petrogenesis of the Leucite hills volcanic rocks, Wyoming, Ph.D. thesis, University of Wyoming.

Ohta, T., and H. Arai (2007), Statistical empirical index of chemical weathering in igneous rocks: A new tool for evaluating the degree of weathering, *Chemical Geology*, *240*(3), 280–297, doi:10.1016/j.chemgeo.2007.02.017.

Pawlowsky-Glahn, V. (2015a), Chapter 2: Compositional data and their sample space, in *Modelling and analysis of compositional data*, Statistics in practice, pp. 8–22, John Wiley & Sons, Inc, Chichester, West Sussex, UK.

Pawlowsky-Glahn, V. (2015b), Chapter 9: Compositional Processes, in *Modelling and analysis of compositional data*, Statistics in practice, pp. 172–205, John Wiley & Sons, Inc, Chichester, West Sussex, UK.

Pearson, K. (1897), Mathematical contributions to the theory of evolution.—On a form of spurious correlation which may arise when indices are used in the measurement of organs, *Proceedings of the Royal Society of London*, *60*(359-367), 489–498, doi:10.1098/rspl.1896.0076.

Peters, S. E., and J. M. Husson (2017), Sediment cycling on continental and oceanic crust, *Geology*, *45*(4), 323–326, doi:10.1130/G38861.1.

R Core Team (2018), R: A Language and Environment for Statistical Computing.

Rudnick, R. L. (1995), Making continental crust, *Nature*, *378*(6557), 571, doi:10.1038/378571a0.

Rudnick, R. L., and S. Gao (2003), Composition of the Continental Crust, *Treatise on Geochemistry*, *3*, 659, doi:10.1016/B0-08-043751-6/03016-4.

Sayles, F. L., and P. C. Mangelsdorf (1977), The equilibration of clay minerals with sea water: exchange reactions, *Geochimica et Cosmochimica Acta*, *41*(7), 951–960, doi:10.1016/0016-7037(77)90154-5.

Simon, L., and C. Lécuyer (2005), Continental recycling: The oxygen isotope point of view: CONTINENTAL RECYCLING, *Geochemistry, Geophysics, Geosystems*, *6*(8), n/a–n/a, doi:10.1029/2005GC000958.

Straume, E. O., C. Gaina, S. Medvedev, K. Hochmuth, K. Gohl, J. M. Whittaker, R. A. Fattah, J. C. Doornenbal, and J. R. Hopper (2019), GlobSed: Updated Total Sediment Thickness in the World's Oceans, *Geochemistry, Geophysics, Geosystems*, *20*(4), 1756–1772, doi:10.1029/2018GC008115.

Tang, M., K. Chen, and R. L. Rudnick (2016), Archean upper crust transition from mafic to felsic marks the onset of plate tectonics, *Science*, *351*(6271), 372–375, doi:10.1126/science.aad5513.

Taylor, S. R. (1985), *The continental crust: its composition and evolution, an examination of the geochemical record preserved in sedimentary rocks*, Geoscience texts, Blackwell Scientific, Oxford.

van den Boogaart, K. G., R. Tolosana, and M. Bren (2015), compositions: Compositional Data Analysis.

Vermeesch, P., and E. Garzanti (2015), Making geological sense of 'Big Data' in sedimentary provenance analysis, *Chemical Geology*, *409*, 20–27, doi:10.1016/j.chemgeo.2015.05.004.

Viers, J., B. Dupré, and J. Gaillardet (2009), Chemical composition of suspended sediments in World Rivers: New insights from a new database, *Science of The Total Environment*, *407*(2), 853–868, doi:10.1016/j.scitotenv.2008.09.053.

von Eynatten, H., C. Barceló-Vidal, and V. Pawlowsky-Glahn (2003), Modelling Compositional Change: The Example of Chemical Weathering of Granitoid Rocks, *Mathematical*

Geology, *35*(3), 231–251, doi:10.1023/A:1023835513705.

von Eynatten, H., R. Tolosana-Delgado, and V. Karius (2012), Sediment generation in modern glacial settings: Grain-size and source-rock control on sediment composition, *Sedimentary Geology*, *280*, 80–92, doi:10.1016/j.sedgeo.2012.03.008.

von Eynatten, H., R. Tolosana-Delgado, V. Karius, K. Bachmann, and L. Caracciolo (2016), Sediment generation in humid Mediterranean setting: Grain-size and source-rock control on sediment geochemistry and mineralogy (Sila Massif, Calabria), *Sedimentary Geology*, *336*, 68–80, doi:10.1016/j.sedgeo.2015.10.008.

Wedepohl, K. H. (1995), The composition of the continental crust, *Geochimica et Cosmochimica Acta*, *59*(7), 1217–1232, doi:10.1016/0016-7037(95)00038-2.